Math. Struct. in Comp. Science (2007), *vol.* 17, *pp.* 1–39.
doi:10.1017/S0960129506705944 Printed in the United Kingdom

The discrete versus continuous controversy in physics

ANNICK LESNE

LPTMC UMR7600, Université Pierre et Marie Curie-Paris 6,
4 place Jussieu, F-75252 Paris
And:
Institut des Hautes Études Scientifiques,
35 route de Chartres, F-91440 Bures-sur-Yvette, France
Email: lesne@ihes.fr

Received 27 October 2004; revised 28 January 2006

This paper presents a sample of the deep and multiple interplay between discrete and continuous behaviours and the corresponding modellings in physics. The aim of this overview is to show that discrete and continuous features coexist in any natural phenomenon, depending on the scales of observation. Accordingly, different models, either discrete or continuous in time, space, phase space or conjugate space can be considered. Some caveats about their limits of validity and their interrelationships (discretisation and continuous limits) are pointed out. Difficulties and gaps arising from the singular nature of continuous limits and from the information loss accompanying discretisation are discussed.

Contents

1. Introduction: setting the stage

This special issue of *Mathematical Structures in Computer Science* reflects the deep and multiple debates arising in pure and computational mathematics that concern discrete *versus* continuous frameworks and computations. The issues under debate range from practical caveats about the use of discrete computational schemes for solving continuous equations, or continuous frameworks to describe discrete systems, through to conceptual questions about the very nature, either discrete or continuous, of reality (not just our perception of reality). The tension between discrete and continuous aspects is also ubiquitous in physics. In this contribution, I will try to give a brief, though inevitably far from complete, account of the numerous facets of this dilemma from a physical viewpoint, with as few prerequisites as possible.

1.1. *The terms of the debate: 'discrete' and 'continuous'*

We will begin by clarifying the issues and sketching a skeleton on which specific examples will be built. The first step is to agree on the terms of the debate. The words discrete and continuous can refer to:

Time: The evolution of a system can be described either as a continuous trajectory in the space of system states (what is called the 'phase space'), or as a discrete sequence of successive states (see Section 2).

Real space: The underlying space (of dimension $d = 1, 2, 3$ in natural situations or possibly larger in theoretical case studies) might be seen either as a continuum, where positions

are labelled by d real-valued coordinates or as a tiling of discrete cells, or, equivalently, as a lattice, where positions are labelled by d integers (see Section 3).

Phase space: The representation of the system state may scan a continuum (a vector space or a manifold) or vary within a discrete set (finite or countable) of configurations (see Section 4).

Conjugate space (in the context of spectral analyses): We shall see in Section 5 that spectra offer another modality to the 'discrete *versus* continuous' dichotomy.

Note that the meaning of 'continuous' is less ambiguous in physics than in mathematics, where set-theoretic, topological and measure-theoretic notions of continuity are superimposed. In physics, the required smoothness is included in the very notion of a continuous medium, and in the same way, a continuous dynamical system will be differentiable unless explicitly stated to be otherwise. It may seem sensible to distinguish between *discrete* systems, namely those made of disjoint (seemingly intrinsic) particles, and *discretised* systems, resulting from a (seemingly arbitrary) partition. However, the examples of quantum particles, localisation and pattern formation (Section 3), and symbolic dynamics (Section 4) will show that such a distinction may, in fact, be irrelevant.

1.2. *The debated questions*

The debate itself takes place at different levels:

— It might concern *computational techniques*, for instance, discrete numerical schemes used to implement continuous equations, or continuous limits replacing an exact discrete formula by an approximate but tractable one.

— It might refer to the choice of the *proper framework to model* the system according to the phenomenon of interest and the description (or observation) scale.

— Finally, it might consider the *nature of the phenomenon*, and investigate the observable consequences of the discrete nature of any actual material (made of atoms) and the quantum nature (discrete low-energy levels) of these atoms or, on the other hand, investigate whether the underlying continuous wave function of the system is essential to understanding its behaviour.

This third facet of the debate partly vanishes in the now generally accepted ambivalent picture of, say, an electron viewed *jointly* as a particle and as a wave, and we will see that similar ambivalent pictures are also the rule at larger scales in classical physics.

2. Discrete *versus* continuous in time

In this section I present some examples illustrating the relationships between discrete-time and continuous-time dynamic modellings. The focus will be on difficulties that can arise, in theoretical modelling (Sections 2.1, 2.2, 2.3), data analysis (Section 2.4) or numerical implementation (Section 2.5), when trying to form a bridge between the discrete and continuous viewpoints.

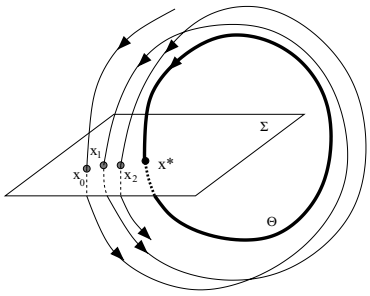

Fig. 1. Poincaré section discretisation method. The periodic orbit $\mathcal{O}$ is underlined in bold. The successive intersections x_0, x_1, x_2,... of a continuous trajectory with the section Σ define the return map φ_Σ through $x_1 = \varphi_\Sigma(x_0)$, $x_2 = \varphi_\Sigma(x_1)$, and so on.

2.1. *Poincaré sections*

A generally accepted example of a discretisation procedure for a continuous dynamical system is provided by Poincaré sections (see Figure 1). This procedure was devised by Poincaré in the context of celestial mechanics, with the aim of reducing the analysis of long-term planetary motion and its dynamic stability (Poincaré 1892).

Let us consider an autonomous differentiable dynamical system $\dot{z} = V(z)$, generating a flow $\Phi(z,t)$ and possessing a *periodic orbit* $\mathcal{O}$ of period T. The behaviour of the flow in the neighbourhood of $\mathcal{O}$ can be tracked through the successive intersections of the flow with a hypersurface Σ (for instance, the locus of points sharing a common phase) crossing $\mathcal{O}$ *once and transversally* at $x^* \in \Sigma$. One thus defines the *return map* φ_Σ (or *Poincaré map*) in an appropriate neighbourhood U of x^* in Σ: the point $x_1 = \varphi_\Sigma(x_0)$ is the first intersection with Σ of the trajectory $t \to \Phi(x_0,t)$ starting from $x_0 \in U$, and the time $\tau(x_0)$ at which the intersection occurs (that is, such that $\Phi(x_0,\tau(x_0)) = \varphi_\Sigma(x_0) = x_1$) is called the *return time* (Guckenheimer and Holmes 1983). By construction, $\varphi_\Sigma(x^*) = x^*$, that is, x^* is a fixed point of the Poincaré map and $\tau(x^*) = T$.

The rationale for this discretisation is the qualitative similarity between the behaviour of the discrete evolution generated by φ_Σ in Σ behaviour of the original (continuous) flow, in particular, with regard to the stability of the periodic orbit $\mathcal{O}$, which is identical to the stability of its trace x^* under the action of the Poincaré map φ_Σ. The correspondence is even quantitative, as we shall see now. Linearising the continuous dynamical system $\dot{z} = V(z)$ around the periodic orbit $\mathcal{O}$ yields an equation $\dot{u} = DV[\Phi(z,x^*)].u$ whose solutions are of the form $u(t) = u_0(t)e^{tR}$, with $u_0(t+T) = u_0(t)$ for any t and R a matrix. The eigenvalues $(\Lambda_j)_j$ of the constant matrix e^{TR} are called the *Floquet multipliers* of the orbit $\mathcal{O}$. The multiplier associated with perturbations along the orbit $\mathcal{O}$ is $\Lambda_0 = 1$; the moduli of the remaining ones determine the stability of $\mathcal{O}$ (stable if all are smaller than 1). It is straightforward to show that the eigenvalues $(\lambda_j)_j$ of the Jacobian matrix $D\varphi_\Sigma(x^*)$ of φ_Σ in x^* (also called the stability matrix of the fixed point x^*) are related to the Floquet multipliers by the equation $\Lambda_j = e^{\lambda_j T}$ (with $\Lambda_0 = 1$) (Guckenheimer and Holmes 1983): the (in)stability of x^* with respect to the discrete Poincaré dynamics is thus equivalent to the (in)stability of the periodic orbit $\mathcal{O}$ with respect to the original continuous dynamics. The multipliers $(\Lambda_j)_j$ are characteristics of the periodic orbit as a whole, and hence do

not depend on the specific intersection point x^*; in consequence, *changing the section* Σ *would not modify the exponents* $(\lambda_j)_j$, *or the stability properties derived from the analysis of the discrete dynamics.*

In this method, the discretisation step is not chosen arbitrarily but prescribed by the dynamics. The main virtue of a Poincaré section is, indeed, that it provides an *intrinsic discretisation*, lowering the phase space dimension by at least one unit, that is adapted to the dynamics (the time step $\tau(x_0)$ depends on the trajectory considered). It captures some *generic features* of the continuous flow, for example, perturbations modifying trajectories outside Σ are of no consequences if the intersections with Σ are preserved. It is thus a first step in bringing out the geometry of the dynamics and its universal properties.

An important caveat is the *restricted range of validity* (in the phase space) of this discretisation: the return map is defined only in a neighbourhood U of the periodic orbit $\mathcal{O}$ (which should intersect Σ once only). Smoothness of the flow in U is also essential. This is usually satisfied, ensuring a wide range of application of the Poincaré section method, but in some special instances, it may happen that the return time $\tau(x)$ is not bounded above and below in U, and the Poincaré map then fails to reflect quantitatively the behaviour of the flow: if $\tau(x)$ does not remain in a finite interval $[\tau_m, \tau_M]$ (with $\tau_m > 0$ and $\tau_M < \infty$) for any $x \in U$, the time correlation functions of the discrete and continuous flows differ strongly, and, accordingly, their Fourier transforms (which are called power spectra, see Section 5.3) exhibit different behaviours. For instance, the divergence of $\tau(x)$ makes the correlation time of the continuous flow diverge even if the correlation function of the discrete evolution is well-behaved, that is, decreases exponentially with a finite characteristic time. The way out of this difficulty is to keep track of the return time function $x \to \tau(x)$. To this end, a new mathematical object has been introduced, which is known as a *special flow* (or 'flow under the function $\tau(x)$', or 'flow over the map $\varphi_\Sigma(x)$'). It is a continuous-time dynamics $[x(t), y(t)]$, with a step-wise constant component $x(t)$ (associated with the Poincaré map) varying in the Poincaré section Σ and another function $y(t)$ taking real positive values. It is defined recursively as follows:

— Starting from $(x_0, 0)$ at time $t = 0$, the second component y steadily increases with velocity 1 until it reaches the value $\tau(x_0)$, at time $t = \tau(x_0)$.
— The trajectory then jumps from $[x_0, \tau(x_0)]$ to the point $[x_1 \equiv \varphi_\Sigma(x_0), 0]$.
— The second component then steadily increases with velocity 1 until it reaches the value $\tau(x_1)$, at time $t = \tau(x_0) + \tau(x_1)$.
— The trajectory then jumps from $[x_1, \tau(x_1)]$ to the point $[x_2 \equiv \varphi_\Sigma^2(x_0), 0]$, and so on.

Such a flow forms a bridge between the dynamics generated by the Poincaré map, which is too reduced in the singular cases considered here, and the original continuous one: the spectral properties (that is, time correlations) of the special flow matches those of the continuous dynamics (Zaks and Pikovsky 2003).

2.2. *Billiards and Birkhoff maps*

A special instance of Poincaré maps is encountered in billiards (see Figure 2). The motion of a tracer point-particle inside the billiard is an alternation of free flights and elastic

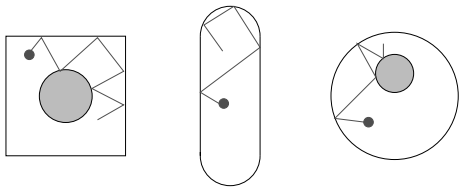

Fig. 2. Three examples of chaotic billiards: (left) Sinai's billiard, (middle) Bunimovich's stadium, (right) when the outer square wall of the Sinai's billiard is replaced by a circular wall, the inner disk should be eccentric in order to get chaos.

reflections on the boundaries: consequently, the phase space has dimension $d = 3$ for a billiard in the plane, since the modulus of the particle velocity remains constant. The dynamic recursion is fully determined by a knowledge of the collisions, namely, by the map relating a pre-collision state to the next one, which is known as the *Birkhoff map* (Gaspard 2004a). This corresponds to the Poincaré map associated with the section containing the particle states $\{(\vec{r},\vec{v})\}$ with $\vec{r}$ located on the boundary and $\vec{v}$ the incoming velocity. The return time is equal to the free flight duration, and hence depends on the overall shape of the billiard (in general, on the boundary point where reflection occurs). The Birkhoff map critically depends on the local geometry of the boundary: for instance, a convex boundary (for example, a disk) is defocusing and amplifies any incident inhomogeneity or fluctuation, generically leading to chaos if iterated in a bounded domain, as in the Sinai's billiard represented in Figure 2 (left).

2.3. *Discrete models*

Discrete models can also be introduced directly, for instance in population dynamics, where each time label corresponds to a generation. Let us consider the formal example $x_{n+1} = x_n + hg(x_n)$ in order to underline a key point: the comparison with a continuous counterpart $dx/dt = ag(x)$ over a duration h_0 shows that the parameter $h = ah_0$ accounts for both the instantaneous growth rate a and for the delay h_0 that takes place between the action $ag(x_n)$ and its consequence on the following state x_{n+1}. It is thus not surprising that h appears as a control parameter of the behaviour. Oscillations might appear at large enough values of h if g is non-linear – typically when the delay h_0 overwhelms the characteristic growth time $1/a$. This point is worked out for detailed examples in the contribution by H. Krivine *et al.* in this volume, where it is shown to give a qualitative, and even a quantitative, understanding of the instabilities arising in the numerical (hence discrete) implementation of continuous dynamics (see also Section 2.5).

More generally, it should be borne in mind that dynamical system modelling, for example, for chemical reactions, accounts for time lags *through kinetic rates of memoryless evolution equations*. This is technically most fruitful, but might sometimes erase the actual mechanisms, for example, the interplay between delays and characteristic times, or the kinetic race between competing chemical pathways. Alternative approaches have been developed, such as delay equations, integro-differential equations involving a memory kernel, or a logical circuit analysis (Thomas and Kaufman 2001), which is technically more tractable for complex systems.

2.4. *The Nyquist theorem on experimental sampling frequency*

On the experimental side, concrete bounds imposed by time resolution of the recording apparatus are described by an important theorem of signal analysis: the *Nyquist theorem* (Nyquist 1928; Shannon 1949). Sampling frequency puts a limit on the variations that can be followed: it is obvious that variations occuring faster than the sampling frequency, hence taking place between two successive recordings, cannot be tracked. The Nyquist theorem makes this quite intuitive statement quantitative: *a full experimental determination of a time signal $f(t)$ containing no frequencies higher than ω_m requires us to sample the signal with a time resolution $\tau \leqslant \tau_m = \pi/\omega_m$*. To be more precise, the case of discrete sampling (when the apparatus needs to relax between successive measurements) should be distinguished from the case of local averaging (when the overwhelming lag comes from the time integration performed by the apparatus to deliver a value), which is reflected in a factor of 2 in the above bound.

2.5. *Euler discretisation schemes*

Numerical resolution of continuous equations $dX/dt = g(X)$ is generally implemented using finite difference methods, such as the (first-order) *Euler discretisation scheme* $x_{n+1} = x_n + hg(x_n)$ with $x_n \approx X(t_n = nh)$. In this numerical analysis context, the relation between discrete-time and continuous-time dynamics is well controlled and harmless provided the continuous evolution has characteristic times bounded below by $2\tau_m$ and the discretisation step h remains below τ_m, in agreement with the Nyquist theorem (see Section 2.4). Higher-order schemes involve a higher-order Taylor expansion of the (integrated) continuous evolution law $X(t_n + h) = X(t_n) + \int_0^h g[X(s)]ds$, leading to the following recursion at order 2: $x_{n+1} = x_n + hg(x_n) + h^2 g(x_n)g'(x_n)/2$. Using these higher-order schemes allows us to relax the bound h_c on the time step up to which the numerical scheme is 'stable', in the sense that its discrete-time solution interpolates the continuous one. The stability threshold $h_c(n)$ of the Euler scheme of order n increases with n up to infinity. Implicit schemes can be used to cure the numerical instability of direct schemes (they actually correspond to a direct scheme of infinite order): basically, the idea is to solve the recursion $x_{n+1} = x_n + hg(x_{n+1})$ instead of $x_{n+1} = x_n + hg(x_n)$ in order to reconstruct the continuous solution of $dX/dt = g(X)$. The price we pay is that these implicit schemes are far less tractable numerically. A basic example is detailed in the contribution by H. Krivine *et al.* in this volume. Another well-known example of misleading discretisation is provided by the Verlet time-discretisation for the pendulum: one obtains the standard map ($I_{n+1} = I_n + K \sin\theta_n, \theta_{n+1} = \theta_n + I_{n+1}$) whose control parameter K is proportional to the discretisation step h. For $h > h_c$, it is chaotic, while the original system is regular.

3. Discrete *versus* continuous in real space

The discussion about discrete or continuous time variables presented in the previous section should naturally be supplemented with a similar discussion regarding real-space variables. Issues range from the nature of a particle (Sections 3.1 and 3.7) to the status

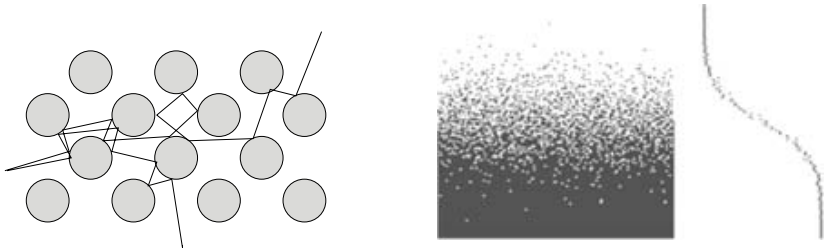

Fig. 3. (Left) microscopic deterministic model of diffusive transport (the Lorentz gas model, which was initially developed as a classical model of electron transport in the lattice formed by the atomic nuclei (Dorfman 1999)) where a light particle experiences numerous elastic collisions on circular scatterers (grey disks). The defocusing character of the collisions induces molecular chaos, in turn generating a diffusive motion and supporting a statistical approach. (Right) observation at time t of the microscopic simulation (implementing discrete random walks) of diffusion in a semi-infinite box, starting from a step in $x = 0$ at time 0. (Extreme right) average profile $n(x,t)$ (vertical axis represents the spatial coordinate x whereas concentration $n(x,t)$ spans values from 0 to 1 horizontally); $n(x,t)$ tends to the solution of the 1-dimensional diffusion equation $\partial_t n = \partial^2_{xx} n$ as the number of particles tends to infinity.

of lattice models (Section 3.2), caveats about continuous limits (Sections 3.3 and 3.4), and the origin and modelling of localisation (Sections 3.5 and 3.6).

3.1. *From molecular chaos to continuous media*

In classical physics, an important paradigm bridging the discrete structure of any material made of atoms or molecules and a continuous description is the *continuous medium approximation*. It corresponds to a mesoscopic modelling of a many-particles system extended in space, for instance a fluid, starting with a partition of the real space into cells of linear size a (it is noticeable that the passage from a cloud of particles to a continuous medium begins with a real-space discretisation). The main assumption is that a is large compared to the microscopic scales (for example, the mean free path of the molecules), but small compared to the macroscopic scales (for example, the characteristic length associated with density or temperature gradients). In particular, each cell should contain a large number of particles: $\rho a^d \gg 1$ if ρ is the number density of the fluid and d the real-space dimension. An argument based on the law of large numbers, itself rooted in an assumption of molecular chaos preventing long-range correlations between the molecules (see Figure 3), supports a continuous description of the medium at the cell level: any observable $\mathscr{A}$ will be associated with a *smooth* and *deterministic* field $A(\vec{r},t)$, where $A(\vec{r},t)$ is the value of $\mathscr{A}$ averaged at time t over the cell located in $\vec{r}$. For instance, in hydrodynamics, A will be the density, velocity or temperature field (Landau and Lifschitz 1984).

This description emerges from a full statistical picture describing the N-particle system through its distribution function f_N such that

$$f_N(\vec{r}_1,\vec{v}_1,\ldots,\vec{r}_N,\vec{v}_N,t)d^d\vec{r}_1 d^d\vec{v}_1 \ldots d^d\vec{r}_N d^d\vec{v}_N$$

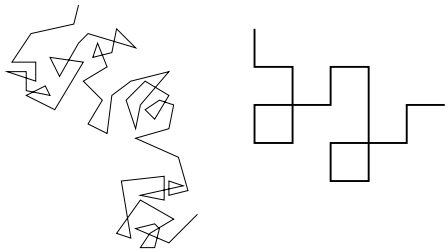

Fig. 4. Lattice approximation (right) of a Brownian trajectory (left). The associated dynamic model is a lattice random walk (Markov chain) fully prescribed by the probability of jumping from any node to one of its nearest neighbours on the lattice.

is the probability that for each $j = 1, \ldots, N$, the particle j lies in the elementary volume $d^d\vec{r}_j \sim a^d$ around $\vec{r}_j$ with a velocity lying in the elementary volume $d^d\vec{v}_j$ around $\vec{v}_j$ (where again d is the dimension of the real space, that is, normally $d = 3$). The time evolution of this distribution function is ruled by the Liouville equation following from the deterministic Newtonian dynamics for the N particles. The following steps are to integrate over $N - 1$ particles, then to use the Boltzmann approximation

$$f_2(\vec{r}_1, \vec{v}_1, \vec{r}_2, \vec{v}_2, t) \approx f_1(\vec{r}_1, \vec{v}_1) f_1(\vec{r}_2, \vec{v}_2)$$

(again supported by the decorrelation achieved by molecular chaos) to express the evolution of $f_1(\vec{r}_1, \vec{v}_1)$ in a closed form (that is, involving only f_1), and, finally, integrating out the velocity $\vec{v}_1$ to get the density $n(\vec{r}, t)$ and the velocity field $\vec{u}(\vec{r}, t)$ (Dorfman 1999)

$$n(\vec{r}, t) = \int f_1(\vec{r}, \vec{v}) d^d\vec{v}, \qquad \vec{u}(\vec{r}, t) = \frac{1}{n(\vec{r}, t)} \int \vec{v} f_1(\vec{r}, \vec{v}) d^d\vec{v} \tag{1}$$

and the temperature

$$T(\vec{r}, t) = \frac{1}{d\, k_B\, n(\vec{r}, t)} \int \frac{mv^2}{2} f_1(\vec{r}, \vec{v}) d^d\vec{v}. \tag{2}$$

This description is generally supplemented with a hypothesis of *local thermodynamic equilibrium*, in each cell, allowing us to use all the thermodynamic relations at each point $\vec{r}$. The simplest example is the description of transport phenomena, for example, the diffusion equation $\partial_t n = D\Delta n$ (where Δ denotes the Laplacian) starting from deterministic molecular dynamics (Laguës and Lesne 2003). Work is still in progress to extend such an effective continuous mesoscopic description to far-from-equilibrium systems, the main open issue being to define entropy and temperature on microscopic bases (Gruber *et al.* 2004).

3.2. *Lattice models*

Conversely, continuous models might be reduced, for example, for computation or simulation purposes, into lattice models, where the underlying real space is a regular lattice. Three major examples are illustrated in Figures 4, 5 and 6, namely, Brownian motion on a lattice, random-walk modelling of polymer chain conformations and percolation theory for, for example, porous media and other disordered systems. We will now consider

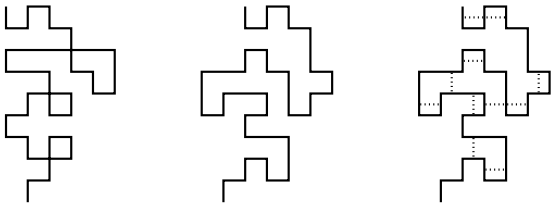

Fig. 5. Lattice models of polymers. (Left) Brownian random walk, with no correlations between successive steps; the size a of a step (a 'monomer') should be larger than the persistence length of the actual polymer chain so that all relative orientations are possible. (Middle) steric hindrance between successive monomers is taken into account in a more refined model, known as *self-avoiding walk*; it exhibits an infinite memory since the walker remembers all the previously visited nodes in order to avoid them. (Right) a third model, the interacting self-avoiding walk, accounts for short but finite range interactions between monomers: self-avoidance (infinite repulsion between monomers at the same point) is here supplemented by an interaction $-J$ (attractive if $J > 0$) between any neighbouring steps (that is, monomers) on the lattice (dotted lines).

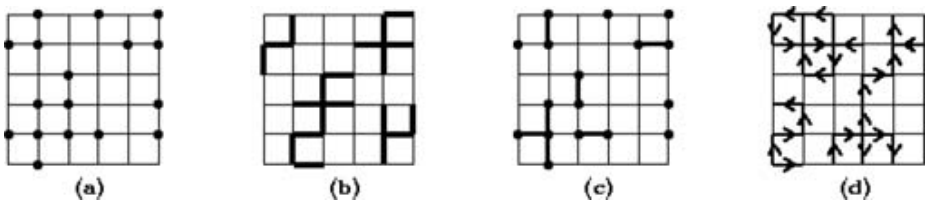

Fig. 6. Percolation models: the real space is discretised, either as a lattice of nodes (a: site percolation), a web of links (b: bond percolation), both (c: site-bond percolation) or as a web of oriented links (d: directed percolation). Each unit (node or link) is supposed to be fully described by a Boolean state variable 0 (empty) or 1 (occupied). Sites are occupied (links are present) with a probability p independently each of each other. Overall behaviour (for example, conductivity, permeability, contagion) depends on the existence of a percolating cluster, namely a connected path bridging the opposite sides of the lattice; its emergence is a critical transition, occurring for a well-defined probability p_c (*percolation threshold*) when lattice size goes to infinity (Stauffer and Aharony 1992).

briefly the main discrepancies arising between lattice models and actual systems, and the situations where lattice models are relevant.

The discretisation is all the more perceptible as the relative size L/a is small (a being the linear cell size and L the linear lattice size). The continuous limit corresponds to $a/L \to 0$. A strong lattice effect might originate from the restricted symmetry properties of the lattice: translational invariance is replaced by invariance under translations of step equal to an integer multiple of a (we here recover the criterion of validity $a \ll L$). Isotropy breaks down and is replaced by invariance under the action of finite groups of rotations (those encountered in the natural lattice structures of crystals).

Using lattice models is especially relevant when investigating *universal properties*, that is, properties common to physical systems of very different natures but sharing the same geometrical properties and symmetries. Let us consider, for instance, percolation models

(see Figure 6). A remarkable feature is the percolation transition, that is, the emergence of an infinite cluster spanning the whole system, above a threshold $p = p_c$. This transition appears to be a close analogue of a second-order phase transition and it accordingly satisfies scaling laws; for instance, the correlation length ξ obeys: $\xi(p) \sim |p - p_c|^{-\nu}$. The value p_c of percolation threshold depends on the lattice geometry (for example, it differs between a square lattice and a triangular lattice), but the exponents involved in the scaling laws, such as ν, depend only on the space dimension and percolation type (Laguës and Lesne 2003). In the same spirit, universal properties of diffusion support its implementation with discrete random walks: the exponent γ involved in the diffusion law $R(t) \sim t^{\gamma/2}$ will not depend on the lattice geometry (provided the lattice remains regular). One may go further and show, using renormalisation methods (Lesne 1998), that *universal properties are identical in continuous systems and in their discretised versions*; the latter will be preferred for obvious reasons of simplicity in theoretical, and even more so in numerical investigations.

3.3. *Diffusion in a porous medium*

As presented in Figure 3, diffusion basically involves the motion of discrete particles. An operational way to get a continuous description of a diffusion process is to cast the behaviour into a phenomenological description involving effective parameters accounting for all microscopic details through their integrated consequences at higher scales. We will consider diffusion in a porous medium. Two situations should be distinguished (Laguës and Lesne 2003):

— The pores have a finite typical size a. The intuitive idea is that at scales far larger than a, the medium can be considered as a homogeneous continuous medium (see Figure 7). Mathematically well-controlled averaging procedures and homogenisation theorems are then available, for example, relating the derivatives of averaged variables and the average derivatives (Bensoussan *et al.* 1978). It is thus possible to derive the spatio-temporal evolution of the locally averaged density (averaged over a representative region, far larger than a pore but still elementary compared to the whole system). The remarkable fact is that it has the same form as the plain diffusion equation. Such a homogenisation procedure thus yields an effective diffusion equation with a reduced diffusion coefficient $D_{eff} < D$ accounting for the obstacles encountered by the diffusing particles (having a diffusion coefficient D in plain solvent).

— The medium exhibits pores at all sizes (fractal substrate). The diffusion is then anomalous: $R(t) \sim t^{\gamma/2}$ with $\gamma < 1$. A relevant theoretical approach is to mimic the medium using a percolation model right at the percolation threshold, then to investigate transport on the (fractal) percolation cluster. A relation can thus be shown, relating the fractal characteristics of the cluster (its fractal dimension d_f and its spectral dimension $d_s \leqslant d_f$) and the exponent of the diffusion law, namely $\gamma = d_s/d_f$.

This example of diffusion in a porous medium illustrates a wide-ranging conclusion: *continuous limits and effective descriptions require characteristic scales to be bounded and their validity range lies far above these bounds.*

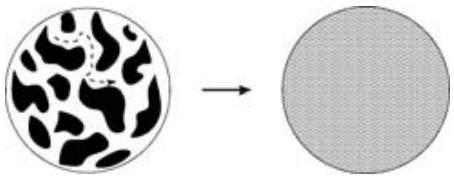

Fig. 7. Homogenisation of a diffusion process in a porous medium: particles, of diffusion coefficient D inside the pores, experience a hampered diffusive motion at larger scales; if the typical size of the pores is finite, normal diffusion is still observed, with lower diffusion coefficient D_{eff}, where D_{eff}/D is related to the medium porosity (Nicholson 2001; Laguës and Lesne 2003).

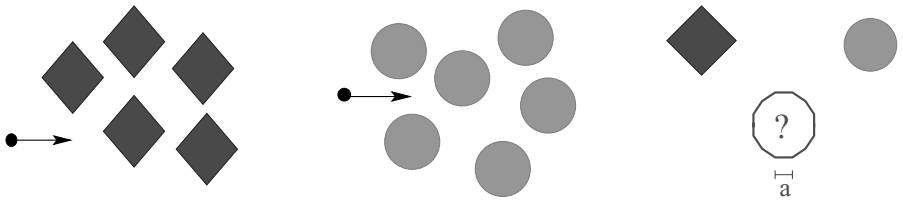

Fig. 8. (Left) wind-tree model where the motion of a tracer is non chaotic. (Middle) Lorentz gas model (see also Figure 3) where the motion of a tracer is chaotic. (Right) what can we say about polygonal scatterers when the facet size a tends to 0?

3.4. *Wind-tree discrete/continuous paradox*

The *Lorentz-gas model* (shown in Figure 3) is an array of circular scatterers amongst which a small tracer particle travels, experiencing elastic collisions at encounters with scatterers. The *wind-tree model* is quite similar, except that disks are replaced by squares (see Figure 8). One can imagine passing from a wind-tree model to a Lorentz gas by considering instead of squares, polygons of constant area and an increasing number of sides (the well-known Archimedian limit towards a circle). It can be shown that the tracer motion is chaotic in a sufficiently dense and generic Lorentz gas (at low densities or in special geometries, the tracer would escape along a free flight without experiencing any collisions). By contrast, the motion is not chaotic for any polygonal wind-tree model, so how can we match these behaviours when the polygons are physically indiscernible from disks? Physically, the puzzle is solved when looking at relevant (large enough) scales: in both models, the tracer exhibits a diffusive motion. Mathematically, the way out of this paradox requires the introduction of an intermediate notion, which is adapted to the resolution ϵ, here in real space: this is the ϵ-entropy (Boffetta *et al.* 2002). The precise definition is given in Section 4.4: it is a time entropy measuring the rate at which observation of the motion with an accuracy ϵ generates information about the trajectory. Its behaviour with respect to ϵ determines the nature of the motion: $\lim_{\epsilon\to 0} h(\epsilon) = h > 0$ for chaotic motion and $h(\epsilon) \sim 1/\epsilon^2$ for Brownian motion. In the case of an array of polygons of side a, the tracer motion looks regular at scales $\epsilon < a$, as reflected by the values $h(\epsilon) \approx 0$, but it looks chaotic at scales $\epsilon > a$, according to the values $h(\epsilon) \approx const > 0$, and even diffusive at scales $\epsilon \gg a$, corresponding to a behaviour $h(\epsilon) \sim 1/\epsilon^2$.

3.5. *Localisation and pattern formation*

Pattern formation, namely the spontaneous appearance of well-defined shapes and patterns in an initially homogeneous system, is ubiquitous in the natural sciences (Cross and Hohenberg 1993; Murray 2002). The emergence of discrete shapes and localised structures relates this issue to our main topic. One of the lessons of pattern formation studies, supplemented by the development of minimal models, such as the set of two coupled reaction–diffusion equations introduced by Turing as a model of morphogenesis (Turing 1952), is that *localisation often follows from collective effects extended in space*. It is the very presence of a spatially extended reactive substrate and non-linear interactions that lead to a phenomenon highly localised in space and seemingly involving only a tiny, almost discrete region of the system. For instance, the stripes observed in Turing structures (corresponding to roughly step-like concentration profiles for the two reactive chemical species) are actually *discrete features of an interacting whole*, and they are indissolubly linked together: it is impossible to isolate, or even to modify one band without modifying another one, and the system can only be regulated as a whole. Such an example illustrates the ambivalent nature, both discrete (in their expression) and continuous (in their mechanisms) of most dynamic patterns encountered in the natural sciences.

3.6. *Localisation and the Dirac 'generalised function'*

On a more abstract level, localisation provides a tractable example of the mathematical idealisation commonly at work in physical modelling. Point particles or the position of some event spatially localised in x_0 are commonly described by a Dirac 'function' $\delta(x - x_0)$. It is actually a generalised function, which is well defined in the framework of the theory of distributions developed by Schwartz. Its physical meaning follows from the limiting behaviour (weak convergence) of peaks of increasing height, decreasing width and constant area:

$$\delta(x - x_0) = \lim_{a \to 0} \frac{1}{\sqrt{2\pi a}} e^{-\frac{(x-x_0)^2}{2a}}. \tag{3}$$

In practice, a unimodal distribution centred in x_0 can be identified with $\delta(x - x_0)$ provided its width satisfies $a \ll \delta x_{obs}$ where δx_{obs} is the experimental resolution. The Dirac distribution is the mathematical idealisation of 'point mass', which is so often used in physics. Its interest for physicists is to endow physical reasoning with mathematical rigour. From a mathematical viewpoint, its achievement is to unify entities with seemingly different mathematical natures (functions and measures) within a comprehensive theory, in which objects are defined, not in themselves, but through their actions on 'probes', namely test-functions (the basic idea of weak convergence). Remarkably, this property is shared with our physical access to the real world.

Another example is provided by the time analogue of a point mass, namely an *instantaneous impulse*. This ideal event corresponds to an infinite force applied during a vanishing time duration. This event can be physically realised in the same way, by considering the limiting behaviour associated with a large force applied for a short duration, when the force and the inverse duration tend to infinity in a concerted way, namely with a fixed ratio.

In the same spirit, *non-standard analysis* allows us to handle limiting behaviours in a more transparent way. It suppresses the qualitative gap between finite and limiting quantities arising when taking a limit $\epsilon \to 0$ by introducing an explicit 'extension of the mathematical world', thereby giving a mathematical status to infinitely small quantities, and replacing qualitative shades by a well-defined ordering between these infinitely small quantities (Diener and Diener 1995).

3.7. *Discrete versus discretised systems*

It now appears that there is no reason to make a fundamental distinction between *discrete* and *discretised* systems: an object seems to be intrinsically discrete, even isolated, only if we choose the proper glasses. Let us consider for instance an atom: at very small scales, those of quantum mechanics, this 'particle' is delocalised. This dichotomy even appears in the classical framework: at long time scales, we do not record a single position of the particle but rather the distribution of its probability in the whole space; we might speak of 'the position' of the particle only if the width of this distribution is smaller than the relevant spatial scales (for example, observation scales or interaction ranges). Hence, discrete objects are not really any more 'objective' than an arbitrarily chosen partition of the space into cells.

4. Discrete *versus* continuous in phase space

4.1. *From agent-based descriptions to continuous models*

The relationship between agent-based descriptions, right at the level of individuals, and kinetic continuous-state descriptions is a ubiquitous issue, encountered, for instance, in population dynamics (Auger and Roussarie 1994), and more generally in the study of the emergence of any collective behaviour ranging from granular media (Ernst 2000) to swarms, flocks or societies (Vicsek 2001), and, finally, at a very different scale, in the context of chemical reactions (Arnold 1980). It has been deeply investigated (Kirkpatrick and Ernst 1991; Chopard and Droz 1998; Droz and Pekalski 2004) to support both kinetic theories of intrinsically discrete systems and discrete simulations (cellular automata) of continuous equations. An explicit derivation of such a *relation between a discrete-state microscopic description and a continuous-state macroscopic one* is interesting as it exposes the approximations lying behind kinetic continuous (real-valued) modelling (Givon *et al.* 2004).

As an example, we will give details of the celebrated Lotka–Volterra (predator–prey) model of population dynamics, which is also discussed in the contribution by H. Krivine *et al.* in this volume:

$$\begin{cases} \dfrac{dx}{dt} = x(a - by) \\ \dfrac{dy}{dt} = y(cx - d) \end{cases} \tag{4}$$

where x and y describe the respective populations of preys and predators.

The first assumption is:

(H1) *The spatial homogeneity of the population.*

This is justified if the environment is itself homogeneous and species are free to move and mix. It allows us to neglect any space dependence and to consider only how the prey and predator populations vary in time. Let $X(t)$ and $Y(t)$ be integers describing the respective numbers of preys and predators at time t. In agent-based simulations, it is possible to describe the behaviour of each agent with great detail, but in analytic or cellular automata approaches, only a minimal, birth-and-death modelling is retained and the populations will evolve according to simple probabilistic rules.

The second assumption is:

(H2) *The Markov character of the evolution.*

Even in a continuous-time dynamics, the description implicitly involves a minimum time scale (the 'size' of dt), and the validity of the Markov assumption requires dt to be larger than the 'memory' of the system[†]. The model is thus entirely determined by a transition rate matrix W:

$$\frac{dP(X,Y,t)}{dt} = \sum_{X'} \sum_{Y'} W(X,Y|X',Y')P(X',Y',t) \tag{5}$$

where the sum runs over all positive integers X' and Y', and

$$\sum_{X} \sum_{Y} W(X,Y|X',Y') = 0 \tag{6}$$

to ensure the conservation of probability ($\sum_X \sum_Y P(X,Y,t) = 1$). Equation (5) requires an additional assumption of the differentiability of $t \to P(X,Y,t)$:

(H3) *No jump, bounded transition rates.*

The fourth assumption is:

(H4) *The identification of macroscopic variables with statistical averages* $\langle X \rangle$ *and* $\langle Y \rangle$.

This assumption is the core of the passage from a microscopic model to a macroscopic one. It is straightforward from (5) to write the time evolution of the various moments, for instance,

$$\frac{d\langle X^n \rangle}{dt} = \sum_{X'} \sum_{Y'} \sum_{X} X^n \, W(X,Y|X',Y')P(X',Y',t). \tag{7}$$

At this stage, in order to go further, we must turn to a specific expression of W. At short time scales, it is justified to suppose that:

(H5) *Only single events will occur with a non-negligible rate.*

Hence we consider only the following elementary transitions in W:

— Birth of a prey: $(X,Y) \to (X+1,Y)$, at a rate $a_0 X$.
— Capture of a prey: $(X,Y) \to (X-1,Y)$, at a rate $b_0 XY$.

[†] This memory is related to direct interactions, and should not be confused with the correlation time (a Markov chain can exhibit long-range correlations, in the case of the near-reducibility of the transition matrix).

— Birth of a predator: $(X, Y) \to (X, Y+1)$, at a rate $c_0 XY$.
— Natural death of a predator: $(X, Y) \to (X, Y-1)$, at a rate $d_0 Y$.

From these we get the expression of non-vanishing components of W:

$$W(X+1, Y|X, Y) = a_0 X \quad W(X-1, Y|X, Y) = bX_0 Y \tag{8}$$

$$W(X, Y+1|X, Y) = c_0 XY \quad W(X, Y-1|X, Y) = d_0 Y. \tag{9}$$

Here again the assumption of the population homogeneity is essential: for instance, each prey gives rise with the same rate a_0 to another one. Alternatively, this assumption can be viewed as:

(H6) *Mean-field approximation, neglecting fluctuations.*

Within this approximation, a_0 is, in fact, a mean rate $\langle \tilde{a}_0 \rangle$, averaged over the whole prey population: $\sum_{i=1}^{X} \tilde{a}_0(i) \approx a_0 X$ if $\tilde{a}_0(i)$ is the reproduction rate of the individual i of the prey population. Note that:

(H7) *The temporal fluctuations of the rates are also neglected* (average rates over a year, for instance).

$W(X-1, Y|X, Y)$ automatically vanishes if $X = 0$ (and, similarly, $W(X, Y-1|X, Y)$ if $Y = 0$), hence transitions towards negative values of X and Y are forbidden: the dynamics remains in the acceptable set of positive integers for both X and Y. The last step is to deduce

$$W(X, Y|X, Y) = -a_0 X - b_0 XY - c_0 XY - d_0 Y. \tag{10}$$

The evolution finally gives:

$$\begin{aligned} \frac{dP(X,Y,t)}{dt} \;=\; & a_0(X-1)P(X-1,Y,t) - a_0 XP(X,Y,t) \\ & + b_0(X+1)YP(X+1,Y,t) - b_0 XYP(X,Y,t) \\ & + c_0 X(Y-1)P(X,Y-1,t) - c_0 XYP(X,Y,t) \\ & + d_0(Y+1)(X,Y+1,t) - d_0 YP(X,Y,t). \end{aligned} \tag{11}$$

Now it is possible to write the evolution of $\langle X \rangle$ and $\langle Y \rangle$:

$$\frac{d\langle X \rangle}{dt} \;=\; a_0 \langle X \rangle - b_0 \langle XY \rangle \tag{12}$$

$$\frac{d\langle Y \rangle}{dt} \;=\; c_0 \langle XY \rangle - d_0 \langle Y \rangle. \tag{13}$$

The main assumption appears here: identifying $\langle XY \rangle$ with $\langle X \rangle \langle Y \rangle$. This amounts to:

(H8) *Neglect microscopic correlations* (so this involves a second mean-field approximation).

The justification for this relies on the law of large numbers and the central limit theorem. Actually, the relevant macroscopic variables are not $\langle X \rangle$ and $\langle Y \rangle$, but rather $x = \langle X/N \rangle$ and $y = \langle Y/N \rangle$ where N is some bound on the total population. While $x = \mathcal{O}(1)$, we have $\langle (X/N)(Y/N) \rangle - xy = \mathcal{O}(1/N)$ decreases with the system size, provided microscopic correlations remain short-range and involves only a (small) fixed number of individuals whatever the size N of the total population. This shows that the relative influence of the cross-correlation between X and Y is actually negligible when the population size is

macroscopic. Note finally that $\langle X \rangle$ and $\langle Y \rangle$ are no longer restricted to integer values, and far more than x and y, thus completing the microscopic foundations of the continuous-state macroscopic model (4), with $a = a_0$, $b = b_0 N$, $c = c_0 N$ and $d = d_0$.

This derivation points out all the different hypotheses and approximations underlying continuous chemical kinetics and similar models; it thus clearly delineates the range of validity of the passage from discrete and stochastic elementary dynamics to a continuous and deterministic one at the scale of the whole population. Accordingly, it hints at situations where this procedure may fail. For instance, finite-size effects are likely to affect chemical kinetic equations when only a small number of molecules are involved in the reaction, for example, inside a living cell. It is then essential to account for the actual discrete and stochastic nature of the variables X, and to investigate the influence of what might be called the 'molecular noise', namely the fluctuations $X - \langle X \rangle$ (that is, $X - Nx$). The consequences of such noise increase as the system size decreases, setting a minimal size N_{min} below which the original discrete and stochastic description should be used; they are expected to be specially dramatic near bifurcation points of the deterministic continuous kinetic equations, where the minimal size N_{min} takes macroscopic values (Gonze *et al.* 2002).

Generalising this to spatio-temporal systems has attracted much work in theoretical physics and chemical physics, as illustrated by Arnold (1980), Chopard and Droz (1998) and Cardy (2004). Rigorous mathematical results supporting the above approach and its spatio-temporal analogue can be found in Rezakhanlou (to appear).

4.2. *Partitions of the phase space*

To account for the finite observation accuracy, say ϵ, available on the system state, it is always possible to replace the original continuous phase space $\mathscr{X}$ by a partition $(\mathscr{X}_{\epsilon,\omega})_\omega$ into cells of linear size ϵ. Nevertheless, starting from a deterministic evolution on $\mathscr{X}$ (discrete in time, that is, modelled by a map $f : \mathscr{X} \to \mathscr{X}$), such a partition does not always achieve a simplification of the analysis. Indeed, if the partition is arbitrary, the associated discretisation typically replaces the deterministic model by a stochastic one, since many trajectories come out of a given cell and generally reach several other cells (Givon *et al.* 2004). Discretising the phase space achieves a fruitful reduction of the dynamics to its essential, somehow universal features, in at least two distinct instances (ignoring related cases):

— *Generating partitions*: For these, by definition, a knowledge of the whole sequence $\bar{\omega} = (\omega_n)_n$ of visited cells specifies a unique point x_0, hence a unique trajectory in the continuous phase space $\cap_{n \geqslant 0} \mathscr{X}_{\epsilon,\omega_n} = \{x_0\}$. There is thus no loss of information when describing the evolution at the cell level since $(\omega_n)_{n \geqslant 0}$ and $(f^n(x_0))_{n \geqslant 0}$ are uniquely related (except, possibly, for a countable set of points). This is the basic feature underlying *symbolic dynamics* (Lind and Marcus 1995). For example, the map $f(x) = 2x$ (modulo 1) in $[0, 1]$ is equivalent to the *Bernoulli shift* $\bar{\omega} \to \sigma\bar{\omega}$ with $(\sigma\bar{\omega})_n = \omega_{n+1}$, acting in the space $\{0, 1\}^*$ of binary sequences: $\bar{\omega}(x)$ is the dyadic representation of x: $x = \sum_{i=0}^{\infty} 2^{-(i+1)}\omega_i$. This equivalence is associated with a partition of the phase space into two cells $\mathscr{X}_0 = [0, 1/2[$ and $\mathscr{X}_1 = [1/2, 1[$, namely $\omega_0(x) = 0$ if

$x < 1/2$, $\omega_1(x) = 1$ if $x \geqslant 1/2$, $\omega_n(x) = 0$ if $f^n(x) < 1/2$, and so on (Badii and Politi 1999):

$$\begin{array}{ccc} x \in [0,1] & \Longrightarrow & \bar{\omega} \in \{0,1\}^* \\ \downarrow & & \downarrow \\ f(x) & \Longrightarrow & \sigma\bar{\omega} \end{array}$$

where $\Longrightarrow$ represents the dyadic representation. Such a conjugacy to a Bernoulli shift is a hallmark of fully developed chaos (strong mixing). Work is in progress to extend this viewpoint to multivariate labels (the discrete time n being supplemented by integer labels associated with a partition of real space) in order to get an operational definition of *spatio-temporal chaos*, that is, chaos occurring in spatially extended systems (Mielke and Zelik 2004).

— *Markov partitions*: For these, by definition[†], the possible successor cells of a given cell do not depend on the history (topological Markov property), which is a prerequisite for devising a Markov chain modelling at the cell level. In a more stringent instance, that of the so-called Markov maps (MacKernan and Nicolis 1994), the reduction to a Markov model can be done exactly: the symbolic dynamics is a Markov chain, which is fully characterised by a transition matrix $W_{\omega\omega'} = \text{Prob}(\omega \to \omega')$, with no loss of information compared with the original evolution in the continuous phase space. In other cases, the reduction to a Markov model relies on a *Markov approximation*, which is supported by the intrinsic stochasticity and memory loss of the underlying evolution in $\mathscr{X}$, if it is sufficiently chaotic, namely mixing (Schnakenberg 1976).

As an aside, note that, as in the above example, discretisation of the phase space is generally performed on a model that is already discrete in time. However, we have already encountered a notable exception in Section 4.1 with *birth-and-death processes*, where a Markov chain in $\mathbf{N}^n$ (Gardiner 1983) describes the number, say, of molecules of n different species and involves unit jumps after random waiting times. Another instance of continuous-time and discrete (or countable) state-space process is provided by *Boolean delay equations* (Ghil and Mullhaupt 1985), where the trajectory is an alternation of jumps $0 \to 1$ and $1 \to 0$ at times varying within a continuum.

4.3. *Shannon entropy*

The information available about any phenomenon depends on the observation scale. This obvious statement can be turned into a quantitative tool by exploiting the *notion of (statistical) entropy*, which was introduced by Shannon and allows us to measure the average information gained during the observation. Shannon entropy S is associated with a partition $\mathscr{P} = [\mathscr{X}_i]_{i=1\ldots N}$ of the phase space and a probability distribution $[p_i]_{i=1\ldots N}$ (with $p_i = \text{Prob}[x \in \mathscr{X}_i]$) accounting for knowledge available prior to the observation (Shannon

[†] For instance, if $\mathscr{X} \subset \mathbf{R}$, f admits a Markov partition $(\mathscr{X}_\omega)_{\omega=1\ldots N}$ if for any $\omega = 1,\ldots,N$, we have $f(\mathscr{X}_\omega) = \cup_{\omega'} \eta_{\omega\omega'} \mathscr{X}_{\omega'}$ where $\eta_{\omega\omega'} = 0$ or 1; see Guckenheimer and Holmes (1983) for the definition of Markov partitions in higher dimensions.

1948):

$$S(\mathscr{P}, [p_i]_i) = -\sum_{i=1}^{N} p_i \log p_i. \tag{14}$$

Here $\log(1/p_i)$ measures the 'surprise' at observing a state $x \in \mathscr{X}_i$ rather than lying in any other cell, and hence is taken[†] as a measure of the information gained by observing the macrostate i. S vanishes if one macrostate i has a probability of 1, and is maximal ($S = \log N$) if the N macrostates are equiprobable. Increasing the resolution, that is, splitting the cells $(\mathscr{X}_i)_{i=1\ldots N}$ into finer ones leads to an increase of S (since $-(p + p')\log(p + p') \leqslant -p\log p - p'\log p'$), which agrees with the intuitive statement introducing this section.

Note that Shannon entropy is closely related to the entropy encountered in statistical mechanics. The connection between statisical mechanics and information theory has already been fully developed[‡], mainly by Jaynes (Jaynes 1989). Boltzmann, in his seminal works, which provided the basis of statistical mechanics, adopted a finitist viewpoint through the introduction of a partition of the continuous classical phase space (the positions and velocities of all the particles composing the system). The obvious flaw in this approach is the arbitrariness of the partition: in particular, as for the Shannon entropy, the statistical entropy varies when the partition varies. These difficulties encountered in classical statistical mechanics in giving an absolute definition of statistical entropy vanish at the quantum level, thanks to the discreteness of the states in a quantum system. Statistical entropy is, indeed, *univoquely defined in quantum mechanics* according to $S = -\operatorname{Tr}\hat{\rho}\log\hat{\rho}$, where $\hat{\rho}$ is the density matrix (Wehrl 1978). Coarse-graining procedures can then be developed to relate the full quantum description to classical ones at higher scales. The increase of entropy observed in these procedures reflects the loss of information (about quantum correlations) accompanying the various projections and the reduction of the system description involved in the quantum/classical connection (Balian 2004).

4.4. *ϵ-entropy*

Continuing the theme of information theory, and more specifically the above notion of (Shannon) entropy, it is fruitful to introduce a time entropy measuring the information at the starting point x_0 that is gained when observing its trajectory $(x_j)_{j\geqslant 0}$ with a *finite resolution* ϵ in the phase space associated with some partition $[\mathscr{X}_{\epsilon,\omega}]_\omega$. Using $\bar{\omega}_n = (\omega_0, \ldots, \omega_{n-1})$ to denote an n-step trajectory observed at this level (by construction $x_j \in \mathscr{X}_{\epsilon,\omega_j}$), we define for each $n \geqslant 1$ a Shannon-like time entropy

$$H_n(\epsilon) = -\sum_{\bar{\omega}_n} \operatorname{Prob}_n(\bar{\omega}_n)\log \operatorname{Prob}_n(\bar{\omega}_n). \tag{15}$$

[†] This choice of $\log(1/p_i)$ as a measure of the information content of the macrostate i (that is, the set $\mathscr{X}_i$ of microstates) is uniquely prescribed if we impose relevant behaviour on S: continuity, concavity and subadditivity when considering the intersection of two partitions, which turns into additivity in the case of statistically independent partitions (Wehrl 1978).

[‡] However, this viewpoint is not shared by the whole community: an alternative, dynamic viewpoint is based instead on the chaotic properties of the microscopic dynamics.

The asymptotic rate

$$h(\epsilon) = \lim_{n\to\infty} \frac{H_n(\epsilon)}{n} = \lim_{n\to\infty} [H_{n+1}(\epsilon) - H_n(\epsilon)] \tag{16}$$

is called the ϵ-*entropy* (Kolmogorov and Tikhomirov 1959; Gaspard and Wang 1993; Nicolis and Gaspard 1994). This is, therefore, the rate of information production when observing the evolution with an accuracy ϵ.

This quantity can be defined for both deterministic and stochastic evolutions. It is, moreover, experimentally accessible (Boffetta *et al.* 2002). It characterises the apparent behaviour at scale ϵ. For instance, $\lim_{\epsilon\to 0} h(\epsilon) = h_{KS}$ (Kolmogorov–Sinai entropy) in the case of deterministic chaos, while $h(\epsilon) \sim 1/\epsilon^2$ for Brownian motion (normal diffusion). So the ϵ-entropy should be computed prior to choosing any modelling. Striking applications of the ϵ-entropy as a tool for describing quantitatively the apparent natures, at different scales, of an actual evolution, are given in Boffetta *et al.* (2002). As we have already sketched in Section 3.4 for the example of chaotic diffusion, this indicator allows us to reconcile models that have seemingly different natures (for example, discrete and continuous) but are related through some continuous limit, typically when decreasing some characteristic size a to 0: behaviours at scale ϵ will be the same whatever the value of a, vanishing or not, provided $a < \epsilon$. On the other hand, the behaviour of $h(\epsilon)$ for $\epsilon < a$ will mark out the difference between the model with $a > 0$ and the limiting, idealised one with $a = 0$. For instance, a behaviour $h(\epsilon) \sim 1/\epsilon^2$, in some window for ϵ, supports a stochastic, diffusion-like description at these scales, whatever the actual mechanism at smaller and larger scales.

We have considered here a discrete-time dynamics. The ϵ-entropy can be generalised for continuous-time dynamics into an (ϵ, τ) *entropy* $h(\epsilon, \tau)$, namely the rate of information production when the evolution is observed with an accuracy ϵ and a time-step τ. As with the ϵ-dependence, the τ-dependence of $h(\epsilon, \tau)$ is highly meaningful, allowing us, for instance, to discriminate deterministic evolution ($h(\epsilon, \tau) \sim h_{KS}$ for a chaotic dynamics of Kolmogorov–Sinai entropy h_{KS}) and stochastic processes ($h(\epsilon, \tau) \sim (1/\tau)\log(1/\epsilon)$ for a white noise). See Gaspard and Wang (1993) for a full account of this extended notion and its applications.

As demonstrated in Falcione *et al.* (2003), this discussion allows us to understand a classical decoherence effect that is quite similar to the quantum decoherence effect described in Berry (2001) and Zurek (1995) (see also Section 5.5). Consider a map whose states, that is, x, are continuous: $x_{k+1} = f(x_k)$ on $[0, 1]$. Moreover, suppose that the associated dynamics is chaotic, which is reflected in a positive Kolmogorov–Sinai entropy $h(f) > 0$. Its discretisation with step $a \ll 1$ (discretisation in the phase space) is written

$$z_{k+1} = \mathrm{E}[(1/a)f(az_k)] \equiv g_a(z_k) \tag{17}$$

where E[.] denotes the integral part. This mapping acts within a finite set of states $\{z_k, k = 0, 1, \ldots, \mathrm{E}[1/a]\}$, hence all trajectories are periodic[†] (after a possible transient)

[†] When the dynamics is periodic of period T, it is straightforward to show that $H_n(\epsilon) = H_T(\epsilon)$ for any $n \geqslant T$, and hence $h(\epsilon) = 0$. The same argument applies here, T being the maximal period of the discrete trajectories

and the dynamics is non-chaotic, which is reflected in $h(g_a) = 0$. We here see again the issue, already encountered in Section 3.4, of matching two behaviours that have different natures but are expected to be indiscernible for all practical purposes when $a \to 0$.

First, note that for $\epsilon > a$, the curve $n \to H_n(\epsilon, g_a)$ follows $n \to H_n(\epsilon, f)$ closely as long as the discretisation and ensuing periodicity of the trajectories are imperceptible. This condition puts a bound $n_{max}(a, \epsilon)$ on the observation duration n, which can be estimated as follows: at $n = n_{max}(a, \epsilon)$, the number $\mathcal{N}_n(\epsilon) \sim e^{nh(\epsilon, f)}$ of ϵ-separated trajectories of length n (that is, trajectories of the continuous system that differ from one another by a distance of at least ϵ at some moment between $t = 0$ and $t = n$) is equal to the number (roughly $1/a$) of discrete states:

$$n_{max}(a, \epsilon) \sim \frac{\log(1/a)}{h(\epsilon, f)}. \tag{18}$$

If n_{max} is large enough, the linear part in the curve $n \to H_n(\epsilon, g_a)$ might be sufficiently marked and long enough to estimate $h(\epsilon, f)$ quite accurately. Above n_{max}, the curve $n \to H_n(\epsilon, f)$ tends to the straight line of slope $h(f)$ (that is, $n^{-1}H_n(\epsilon, f)$ tends to $h(f) > 0$), while $H_n(\epsilon, g_a)$ saturates to a constant finite value (roughly equal to $H_{n_{max}}(\epsilon, g_a)$ and of order $\log(1/a)$), reflecting the periodic regime of the discrete dynamics.

Second, adding uncorrelated microscopic noise to the discrete evolution might restore the features of the continuous evolution at large scales $\epsilon \gg a$, in exactly the same way as adding noise to a quantum evolution allows us to recover the chaotic behaviour, if any, of the classical analogue. This can also be seen in the entropic behaviour. Consider the case where the noise amounts to uncorrelated random jumps into neighbouring a-cells, and use h_{noise} to denote the entropy (rate) of this stochastic process. This noise can be fully perceived only at scales $\epsilon > a$, and then

$$h(\epsilon, g_a + \text{ noise}) \approx h_{noise} \qquad (\epsilon > a). \tag{19}$$

As shown in Falcioni *et al.* (2003), if $h_{noise} \gg h(f)$ and $\epsilon \gg a$, the randomness of the superimposed noise restores the complexity of the chaotic continuous dynamics, namely

$$h(\epsilon, g_a + \text{ noise}) \quad \text{with} \quad a = \alpha\epsilon \quad \text{tends to} \quad h(\epsilon, f) \quad \text{as } \alpha \text{ tends to } 0. \tag{20}$$

The explanation lies in the amplification of the microscopic noise by the deterministic dynamics. In simple terms, the dynamic instability still present in the discrete dynamics (before being truncated by the discretisation and the ensuing periodicity) feeds on the noise and propagates its randomness (that is, its entropy) at larger scales in a way reflecting the underlying continuous dynamics. The random events at scale a allow us to bypass the 'taming' of the chaotic behaviour following from the coarse-graining $f \to g_a$, and to recover the full entropic content of the original continuous dynamics at observation scales ϵ that are large compared with the discretisation step $\epsilon \gg a$. The authors finally suggest that chaotic deterministic systems might appear as effective models for randomly

(T is actually finite since there is a finite number of discrete states, and hence a finite number of discrete deterministic trajectories).

perturbed quantum (and hence discrete) motion, when observed at classical scales (Falcioni *et al.* 2003).

The general point to remember is the *importance of superimposed randomness in the inter-relation between continuous and discrete dynamics.*

5. Spectral analyses

5.1. *Introductory overview of the spectral landscape*

The heading 'spectral analyses' covers a large variety of ideas going under the name of a *spectrum.* The purpose of this section is to give a representative sample of their variety to show that spectral analyses form a whole world, where we need to shed light on the choice between the discrete and continuous (here, spectra), which reflect deep differences in the behaviour of the system, and where we may need a richer picture than that provided by a simple dichotomy between two exclusive possibilities. A preliminary classification will help here. Spectra may correspond to:

— Frequencies or, equivalently, time periods (Fourier modes, Section 5.2, and power spectra, Section 5.3);
— Wave vectors or, equivalently, wavelengths (spatio-temporal normal modes, for example, in pattern formation, Section 5.4);
— Energy levels, Section 5.5;
— Correlation times (that is, characteristic times for the decay of correlations, Section 5.6);
— Amplification rates (Lyapunov exponents, Section 5.7);
— Experimentally available spectra and associated spectroscopy methods, Section 5.8.

5.2. *Fourier analysis*

Fourier analysis was introduced by Fourier in 1807 to solve the heat equation $\partial_t T = \chi \Delta T$ for a temperature profile $T(\vec{r})$ (Fourier 1822). It has since been intensively developed, both on the theoretical side (convergence results, for instance) and on the practical side (computational methods to implement Fourier transforms, such as the Fast Fourier Transform algorithm). I shall not dwell on the basic definitions and properties of Fourier transforms but instead discuss its status in the light of the present discrete/continuous debate.

The basic idea is to decompose, say, a real-valued time function $f(t)$ into purely sinusoidal components, namely $A_\omega \cos(\omega t + \phi)$, or, equivalently, $a_\omega \cos(\omega t) + b_\omega \sin(\omega t)$, or, in the complex form, $\widehat{f}(\omega)e^{i\omega t}$ with $\omega \in \mathbf{R}$. If this function $f(t)$ is T-periodic, only the components with $\omega = \omega_1 \equiv 2\pi/T$ and its harmonics, with frequencies $\omega_n = 2\pi n/T$, remain, turning the continuum of possible frequencies into a discrete set: a discrete 'point spectrum' reveals the periodicity of the associated phenomenon.

The extension to spatio-temporal phenomena is fairly straightforward, replacing $e^{i\omega t}$ with $e^{i\omega t - i\vec{q}.\vec{r}}$. A well-known illustration is provided by musical instruments: flute, violin strings ($d = 1$) or drum ($d = 2$). In this case, looking for a solution of the wave equation describing the system behaviour (for example, its response to an excitation) relates frequencies ω and wave vectors $\vec{q}$ through a dispersion relation $\omega = qc$, where c

is the velocity of sound. Boundary conditions (for example, the deformation of a drum membrane should vanish at its boundary) select only one component (and its harmonics) corresponding to the note emitted by the instrument. Playing the instrument mainly amounts to modulating the boundary conditions to get different notes: this is what a violin player achieves with the fingers of his left hand in tuning the emitted sound by varying the length of the string section actually excited by the bow. The differences between different instruments lie in the relative weight of the harmonics, which are reflected in the timbre and can be controlled by the way the string is excited (compare a guitar, a violin, a piano and a harpsichord).

Fourier analysis makes sense only in the case of linear equations; it extends to weakly non-linear equations in a perturbative way, known as *mode coupling theory* (Ma 1976). Non-linear terms induce a coupling between components, and hence generate new frequencies: for instance, the product of $\hat{f}(\omega_1)$ and $\hat{f}(\omega_2)$ contributes to $\hat{f}(\omega_1 + \omega_2)$. It is thus impossible to excite selectively a single frequency (and its harmonics) in a non-linear system; if a single dominant frequency is observed, its origin lies in the dynamics itself and not in the external influences; we shall give details of the emergence of such intrinsic modes in Section 5.4. Finally, we saw in Section 2.4 that time resolution puts bounds on the spectral range that can be scanned experimentally (Nyquist theorem): if the sampling frequency is bounded above by ω_0, only spectral components with $\omega < \omega_0/2$ can be fully determined (Shannon 1949).

5.3. *Power spectra*

A power spectrum is a special instance of Fourier analysis. Given an evolving system, the power spectrum $S_A(\omega)$ of a given observable A is defined as

$$S_A(\omega) = \lim_{T\to\infty} \frac{1}{T} \left| \int_0^T e^{i\omega t} A(t)\, dt \right|^2 . \tag{21}$$

Much can be seen about the system's behaviour in this spectrum. For instance, a chaotic behaviour is associated with a spectrum having a large bandwidth (Eckmann 1981). The period-doubling scenario towards chaos is also called a 'subharmonic cascade' due to the peculiar, dyadic and self-similar structure of the associated spectrum (Lesne 1998). A quasi-periodic motion (and hence with countable spectrum) with three incommensurable frequencies is structurally unstable (Ruelle and Takens 1971), and the weakest perturbation turns it into a chaotic motion associated with a large-bandwidth spectrum. Let us define the auto-correlation[†] function

$$C_A(t) = \lim_{T\to\infty} \left[\int_0^T A(t+s)A(s)\, \frac{ds}{T} - \left(\int_0^T A(t)\, \frac{dt}{T} \right)^2 \right] . \tag{22}$$

The Fourier transform of $C_A(t)$ is $\widehat{C}_A(\omega) = \sqrt{2\pi}\, S_A(\omega)$. This result is sometimes called the *Wiener–Khinchine theorem*. Actually, this theorem has a far stronger version, including an

[†] The power spectrum and correlation function, as written here, are well defined only *in the stationary state*; otherwise, one should consider the two-time correlation function $C_A(t_0, t)$ for the evolution starting in a given out-of-equilibrium state at time t_0.

ergodic-theoretic aspect: it states the equality of $\sqrt{2\pi}S_A(\omega)$ and $\widehat{\mathscr{C}}(\omega)$ where $\mathscr{C}_A(t)$ is now defined as a statistical correlation function:

$$\mathscr{C}_A(t) = \int A(\varphi_t(x))A(x)\mu(dx) - \left(\int A(x)\mu(dx) \right)^2 \tag{23}$$

where μ is an invariant ergodic[†] measure under the action of the flow $\varphi_t(x)$. It is easy to extend the definition of the correlation function $\mathscr{C}_{AB}(t)$ and power spectrum $S_{AB}(\omega)$ to pairs of observables (A, B) with $\widehat{\mathscr{C}}_{AB}(\omega) = \sqrt{2\pi}\, S_{AB}(\omega)$. Assuming the existence of an invariant ergodic measure μ, Ruelle and Pollicott have shown that for a class of chaotic systems, $S_{AB}(\omega)$ is meromorphic in a stripe extending on both sides of the real axis, and the position of its poles does not depend on the observables A and B under consideration. Moreover, these poles are directly related to the asymptotic behaviour ($t \to \infty$) of the correlation function (a property of the Fourier transform). Complex poles of the power spectrum are thus associated with resonances, the so-called *Ruelle–Pollicott resonances*, and the existence of poles arbitrarily close to the real axis prevent an exponential decay of temporal correlations. Accordingly, mixing requires that all poles lie at a finite distance (bounded below) from the real axis; in this case, they contribute to the correlation decay and their imaginary part provides characteristic times (correlation times) of this decay (Ruelle 1986).

A first kind of singular power spectrum is provided by *'continuous singular' spectra*, corresponding to the case when the correlation function does not decay exponentially to 0 but is still integrable (by contrast with the fully correlated periodic dynamics) (Zaks and Pikovsky 2003). The spectrum is then an intricate superimposition of peaks and large band, that is, of discrete and continuous features. Such spectra occur in weakly chaotic dynamics exhibiting a divergence of the correlation time, corresponding to the intermittent persistence of regular motion (for example, laminar transients near an unstable or imaginary fixed point).

Power spectra can exhibit another singular behaviour lying between the discrete and continuous (see Section 6.4), namely a *power-law behaviour*, with no characteristic scale and features at all scales. A celebrated example is turbulence, which involves the real-space analogue $E(q)$ of the power spectrum $S(\omega)$ as a function of the wave vector q. Under assumptions of statistical homogeneity, isotropy and stationarity, it satisfies $E(q) \sim q^{-5/3}$ in a wide range of wave vectors q called the inertial range, where eddies at all sizes develop and dissipation is not yet efficient (Frisch 1995).

5.4. *Normal modes*

Normal mode analysis generalises Fourier analysis to complex frequencies. It basically amounts to performing a *linear stability analysis* of a uniform stationary state, and to

[†] By definition, the pair (f, μ) consisting of a map $f : \mathscr{X} \to \mathscr{X}$ and a measure μ on $\mathscr{X}$ invariant under the action of f is *ergodic* if and only if any invariant subset $A \subset \mathscr{X}$ is of null or full measure, that is, $\mu(A) = 0$ or $\mu(\mathscr{X} - A) = 0$ provided $f^{-1}(A) = A$. Equivalently, (f, μ) is ergodic if and only if any invariant μ-integrable function φ (that is, such that $\varphi \circ f = \varphi$ μ-almost everywhere) is μ-almost everywhere constant (Pollicott 1998).

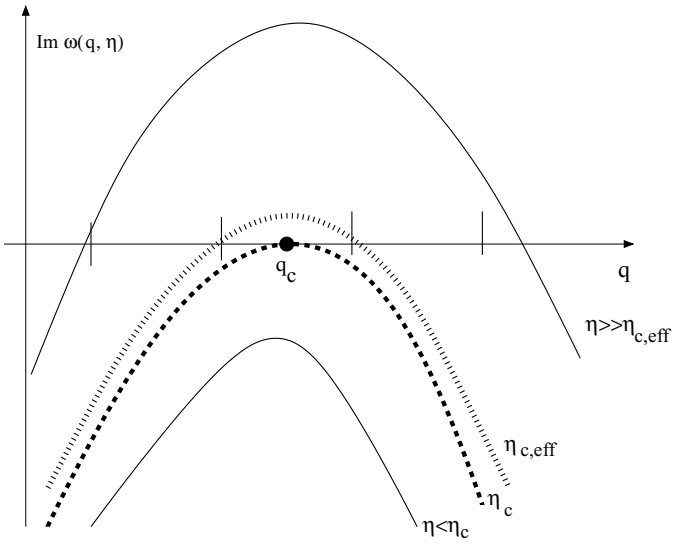

Fig. 9. Dynamic instability and the influence of boundary conditions, requiring that $qL \in 2\pi\mathbf{Z}$ (vertical marks on the q-axis); although the instability appears in q_c for $\eta \geqslant \eta_c$, the actual instability, accounting for boundary constraints, develops only for $\eta \geqslant \eta_{c,eff}$: spectral selection arises in a confined geometry, and might even suppress the dynamic instability.

searching for linear perturbations (solutions of the linearised evolution) with the form

$$a(\vec{q},t)e^{i\vec{q}.\vec{r}} \quad \text{or} \quad A(\omega,\vec{r})e^{-i\omega t} \quad \text{or} \quad \mathscr{A}(\vec{q},\omega)e^{i\vec{q}.\vec{r}i\omega t} \tag{24}$$

yielding a *dispersion relation*

$$\omega = \omega(\vec{q}) \in \mathbf{C} \qquad \text{or more generally} \qquad \mathscr{D}(\omega,\vec{q}) = 0. \tag{25}$$

In a confined medium, $\vec{q}$ is real and 'quantified', as required by the boundary conditions, for example, $qL \in 2\pi\mathbf{Z}$ if the underlying space is an interval $[0, L]$ (as we saw in Section 5.2, the same constraint rules the Fourier spectrum). The mode is stable if and only if $\mathrm{Im}(\omega(\vec{q})) < 0$. The homogeneous stationary state is thus dynamically stable if and only if $\mathrm{Im}(\omega(\vec{q})) < 0$ for any $\vec{q} \in \mathbf{R}^d$.

For simplicity, consider a unidimensional medium of size L, and the situation where its dynamics depends on a control parameter η. Destabilisation occurs at the minimal value η_c such that it exists q_c, with

$$\mathrm{Im}(\omega(\eta_c, q_c)) = 0 \qquad \text{and} \qquad \mathrm{Im}(\omega(\eta_c, q)) < 0 \qquad \text{if} \quad q \neq q_c \tag{26}$$

(see Figure 9). For $\eta > \eta_c$, a continuum $[q_m(\eta), q_M(\eta)]$ of modes is destabilised, surrounding the value $q_c(\eta)$ where $\mathrm{Im}(\omega(q))$ is maximal. In this window, only those wave vectors satisfying

$$qL \in 2\pi\mathbf{Z} \tag{27}$$

are acceptable. *Although the dynamics allows a continuum of unstable modes*[†]*, only a discrete set, selected by the boundary conditions, is actually observed*. It is important to note that the window of unstable modes is independent of the system geometry: boundary conditions intervene later, as a further selection rule fine-tuning specific modes among the set of dynamically unstable ones. Near the instability threshold, or for small system sizes L, the intersection of $[q_m, q_M]$ with $(2\pi/L)\mathbf{Z}$ might be empty: this means that the instability is hindered by the boundary conditions. As sketched in Figure 9, the instability can thus be avoided in a confined geometry (L too small) and it develops only if $\eta > \eta_c(L)$ (or equivalently $L > L_c(\eta)$). On the other hand, in a very extended medium ($L \to \infty$, $2\pi/L \ll dq$), the quantification is almost insignificant and, in practice, one observes a continuum of unstable modes. All this discussion can be substantiated and illustrated using examples of pattern formation (Cross and Hohenberg 1993), such as the celebrated Turing structures (Turing 1952). Spatio-temporal systems thus exhibit the *superimposition of a continuous instability, intrinsically prescribed by the dynamics, and a further selection of discrete modes, imposed by the boundary conditions.*

Note that a continuous symmetry of the evolution equation induces a marginally stable mode $\omega = 0$. Here again a kind of conjugacy appears between continuous features (here a continuous symmetry) and discrete ones (here a mode $\omega = 0$ or $\vec{q} = 0$). However, this conjugacy is neither an opposition nor a negation, but rather a balance, or even a conjunction, where *discrete features exist only when continuous ones are present in the conjugate instance.*

5.5. *Quantum mechanics*

Spectral analysis is at the core of quantum mechanics because of the linear nature of the *Schrödinger equation*

$$\imath\hbar\partial\psi/\partial t = \widehat{H}\Psi \tag{28}$$

and the Hermitian property of the Hamiltonian operator $\widehat{H}$ acting on the wave function ψ. Eigenvalues $(E_k)_k$ of $\widehat{H}$ correspond to energy levels of the system and the associated eigenvectors $(\psi_k)_k$ correspond to 'pure states' of well-defined energy E_k. One distinguishes:

— The case of a *discrete (or pure point) spectrum*, where the spectrum reduces to the set of eigenvalues;
— The opposite situation, which is a *continuous spectrum* with no eigenvalues (and hence no eigenvectors).

However, the normal situation is a *mixed spectrum*, whose restriction to some subspace is a pure point spectrum whereas the complementary part (in the orthogonal, supplementary subspace) is continuous.

The basic idea is that *a discrete spectrum reflects a quantification of the energy*, and hence a non-classical behaviour of the system, while passing to a continuum marks the energy

[†] The modes are *linearly* unstable; in the true dynamics, non-linear effects generally induce a saturation of the instability and turn these unstable modes into well-defined structures of bounded amplitude.

threshold above which the system behaves classically. However, the situation is more complicated than this, and a more refined analysis reveals different kinds of continuous spectra, according to their fine structure (which is related to the existence of 'resonances', namely complex poles of the resolvant [det $(1 - z\widetilde{H}]^{-1}$ of a non-Hermitian extension $\widetilde{H}$ of $\widehat{H}$). This point is described fully for the case of the Helium atom in the contributions by D. Delande and A. Buchleitner in this volume.

An issue that has been investigated quite recently is *quantum chaos*. Here the problem is to determine whether some specific spectral properties are associated with chaotic properties of the corresponding classical system (the limit $\hbar \to 0$, or rather, the limit when the ratio $\hbar/A_c$ tends to 0, where A_c is a classical scale for the action) (Gaspard 2004b). It is important to note that *an isolated quantum system does not exhibit chaos*, even if its classical counterpart is chaotic. The reason is that any fine structure (for example, the homoclinic tangle at the origin of chaos – see the contribution by C. Simo in this volume) in the phase space is bounded below at scale $\hbar$. However, it can be shown that any external influence, even the weakest one, restores the classical chaotic behaviour, a phenomenon belonging to what is called *quantum decoherence* – see, for instance, Berry's introductory paper Berry (2001); see also the classical analogue presented in Section 4.4.

Remarkably, quantum mechanics shows that discrete *versus* continuous issues are multiple and should be precisely delineated to avoid a dialogue of the deaf. Indeed, while quantum systems appear as the discrete counterparts of classical ones with regard to energy spectrum (discrete low-energy levels) and phase space (discrete states), they generally exhibit the opposite behaviour in real space: quantum particles are described by a continuous, spatially extended wave function, while classical ones are localised and described by a few coordinates. This points out that discreteness in phase space[†] and discreteness in real space are not straightforwardly related.

5.6. *Koopman–Frobenius–Perron theory*

Spectral analysis also arises in classical mechanics in association with the *Liouville equation* $\partial_t \rho = L\rho$ for the density $\rho_t(x)$ in the phase space[‡]. This Liouville equation is formally similar to the Schrödinger equation $\partial_t \psi = -\imath \widehat{H}\psi/\hbar$, with the noticeable difference that $\imath\hbar L$ is not Hermitian and ρ is restricted to be a positive function.

You should not be misled by the linearity of this Liouville equation: *it does not mean in any way that the dynamics is linear*; non-linearities of the dynamics are embedded in the evolution of the phase-space dependence of ρ, that is, in the evolution of the relative weight of phase space regions, which can mix in a complicated non-linear way as time goes on.

[†] The discrete or continuous nature of states, that is, the discrete or continuous nature of the energy spectrum, should not be confused with the bounds following from the Heisenberg uncertainty relations, which prevents the simultaneous observation of eigenstates for non-commuting observables, notwithstanding the discrete or continuous nature of their spectra.

[‡] In the case of Hamiltonian dynamics, the Liouville equation takes the form $\partial_t \rho = L\rho \equiv \{H, \rho\}$ where $\{H, \rho\}$ is the Poisson bracket. It follows that $\rho \equiv 1$ is a stationary solution and Hamiltonian dynamics preserves the phase-space volume, a result known as the *Liouville theorem*.

In the case of a discrete time evolution $x_{n+1} = f(x_n)$ in $\mathscr{X} \subset \mathbf{R}^d$, the evolution of the density is given by $\rho_{n+1} = P\rho_n$ where the operator P is called the *Frobenius–Perron operator*. P is linear on $L^1(\mathscr{X}, dx)$, positive ($P\rho \geqslant 0$ if $\rho \geqslant 0$) and preserves the L^1-norm of positive integrable functions. An interesting result is the *relationship to ergodic theory*: in the case when there exists a stationary density ρ^*, the couple (f, ρ^*) is ergodic if and only if $P\rho_n$ is weakly Cesaro-convergent to ρ^*, namely, for any initial density ρ_0 and for any bounded measurable function g,

$$\lim_{n\to\infty} \frac{1}{n} \int \sum_{j=0}^{n-1} P^j \rho_0(x) g(x) dx = \int \rho^*(x) g(x) dx. \tag{29}$$

If $\mathscr{X}$ is of finite measure, (f, ρ^*) is mixing if $P^n\rho_0$ is weakly convergent for any initial density ρ_0, that is, for any bounded measurable function g,

$$\lim_{n\to\infty} \int P^n \rho_0(x) g(x) dx = \int \rho^*(x) g(x) dx. \tag{30}$$

These statements have a spectral counterpart (Parry 1981; Pollicott and Yuri 1998): there exists a stationary density ρ^* if and only if P has an eigenvalue equal to 1 (the eigenvector then being ρ^*); ergodicity follows if and only if this eigenvalue is simple (namely, if and only if ρ^* is the unique stationary density of f). If, moreover, it is an isolated eigenvalue of P, then (f, ρ^*) is mixing. Other eigenvalues are also of interest, since they are associated with characteristic times of the correlation decay. It is here that the close link between Koopman theory and Pollicott–Ruelle resonances (Section 5.3) appears. The Fredholm determinant of P defines the *Selberg–Smale zeta function* $Z(z)$ and the *Ruelle zeta functions* $\zeta_k(z)$:

$$Z(z) = \det(1 - zP) = \prod_k \frac{1}{\zeta_k(z)}. \tag{31}$$

Under some technical conditions (MacKernan and Nicolis 1994), the Ruelle zeta functions can be expressed explicitly from a knowledge of all the periodic orbits $\mathscr{O}_j$ (labelled by j) (Gaspard and Dorfman 1995):

$$\zeta_k(z) = \prod_j \left(1 - \frac{z^{n_j}}{|\Lambda_j| \Lambda_j^{k-1}}\right) \tag{32}$$

where n_j is the period of the periodic orbit $\mathscr{O}_j$ and Λ_j is its stability factor, that is, the product of f' along the orbit, namely $\Lambda_j = f'(x_{j,0}) f'(x_{j,1}) \ldots f'(x_{j,n_j-1})$. Hence, the decay of time correlations (mixing property) of the dynamics is determined by the dynamic behaviour along the periodic orbits; these orbits thus form the skeleton, not only qualitatively but also quantitatively, of the dynamics (see the contribution by C. Simo in this volume). Conversely, the spectrum of P contains the same information, in a somehow integrated form: the inverses of the eigenvalues of U are the poles of $1/Z(z)$ (under some technical restrictions on f). It is notable that the formula (31) (or rather, its inverse giving the expression of $1/Z(z)$) is strongly reminiscent of the semi-classical *Gutzwiller trace formula* bridging the spectrum of the quantum Hamiltonian and some

characteristics (periodic orbits) of the corresponding classical dynamics (Gutzwiller 1990; Gaspard and Dorfman 1995) – see also the contribution by T. Paul in this volume.

5.7. *Lyapunov spectrum*

Given a map f on a compact phase space $\mathscr{X}$ associated with an invariant ergodic measure μ, another spectrum (in addition to the spectrum of the Frobenius–Perron operator and the associated Ruelle–Pollicott resonances described above in Section 5.3 and Section 5.6) can be considered – this is the *Lyapunov spectrum*. The Lyapunov spectrum is a global feature of the flow, and is defined as the spectrum of the asymptotic matrix

$$M = \log \lim_{n\to\infty} [\Lambda_n(x)^\dagger \Lambda_n(x)]^{1/2n} \tag{33}$$

where

$$\Lambda_n(x) = Df[f^{n-1}(x)] \circ \ldots \circ Df(x)$$

is the Jacobian matrix iterated along the flow, for any μ-typical x (note that $M(x)$, being invariant under the action of f, is μ-almost everywhere constant due to the ergodicity of (f, μ)). The dynamics is chaotic if and only if this spectrum has a positive part. This positive part *controls the decay of time correlations* due to chaotic amplification of external noise: correlations decay with time t like $\exp(-t \sum (\text{positive Lyapounov exponents}))$. It is important to note that this decay does not have the same origin as the decay due to mixing associated with the Ruelle–Pollicott resonances (Ruelle 1986) – see Section 5.3 and Section 5.6. This sum of positive exponents provides an upper bound on the Kolmogorov–Sinai entropy, where the bound is conjectured to turn into an equality (the *Pesin equality*) for a large class of dynamical systems, for example, hyperbolic Axiom A systems (Eckmann and Ruelle 1985). Another conjecture, the *Kaplan–Yorke conjecture*, states that the capacity dimension D_0 (roughly, the fractal dimension of the attractor (Baker and Gollub 1996)) is equal to the Lyapunov dimension

$$d_{Lyap} = j + \sum_{i=1}^{j} \lambda_i / \lambda_{j+1} \tag{34}$$

where j is the integer such that $\sum_{i=1}^{j} \lambda_i \geqslant 0$ and $\sum_{i=1}^{j+1} \lambda_i < 0$. This statement has been proved for a two-dimensional hyperbolic mapping where d_{Lyap} reduces to $1 - (\lambda_1/\lambda_2)$. The total sum of this spectrum (trace of M) gives the *average rate of expansion* (or contraction if negative) of the phase-space volume achieved by the dynamics. In the case of Hamiltonian dynamics, this sum is 0; more importantly, under various additional hypotheses (for example, constant kinetic energy), the spectrum satisfies the *pairing property* (Dettmann and Morriss 1996)

$$\lambda_j + \lambda_{2N-j} = 0 \tag{35}$$

where N is the number of degrees of freedom. In the case of extended systems, with many degrees of freedom ($N \gg 1$), the discrete features of the Lyapunov spectrum, especially the step-like structures observed near $\lambda = 0$ (van Beijeren and Dorfman 1995; Taniguchi and Morriss 2002), are still not fully understood. A description of generic scaling properties

with respect to the number N of degrees of freedom and the possible continuous limit of the spectrum after an appropriate rescaling, for example, $\widetilde{\lambda}(\alpha) = \lambda(j = \alpha N)/\lambda_1$, are also still the subject of on-going work.

5.8. *Experimental spectroscopy*

This is not the place even to list the whole variety of spectroscopic methods, which range from infrared spectroscopy to X-rays (that is, from low to high energy), including the still developing fluorescence techniques (which are especially useful in biology for investigations into the functioning of living cells) and more specific probes like circular dichroism (which are sensitive to structural chirality). Spectroscopic methods roughly separate into two classes: *absorption spectra*, where one records how the system selectively absorbs radiation from incident light, and *emission spectra*, where one records the specific wavelengths radiated by the system. In the two cases, the spectrum profile is related to the atomic structure and degrees of freedom through the relation $\Delta E = hv$ between the photon frequency v and the energy jump (towards higher energy during absorption and conversely, towards de-excitation and lower energies during emission). For instance, spectroscopy allows us to identify the elements composing a star from the analysis of its light, or to follow changes in the atomic structure of a macromolecule as some control parameter varies. Its interpretation at larger scale, for instance in terms of conformational changes of the macromolecule, requires a model, and this is one of the purposes and achievements of (computer-assisted) molecular modelling.

5.9. *Some conclusions on spectral analyses*

Spectral analyses provide a powerful method for decomposing a given behaviour into elementary components that are orthogonal to what can be achieved when considering the system at successive instants or when splitting the underlying real space in cells; one speaks of '*conjugate space*'. The discrete/continuous duality appears quite ill-suited to discriminating spectral properties:

— Discrete spectral values have different consequences depending on whether they lie on the real line or in the complex plane.
— Continuous spectra may even be singular (fractal spectra exhibiting a power-law behaviour) and their scaling behaviour discriminates between very different physical behaviours.

The briefest mathematical analysis underlines the fact that the spectrum of any operator is highly dependent on the functional space in which it operates; in physical terms, it depends on the set of observables (in particular, it is prescribed by the geometry and boundary conditions). At the opposite extreme, experimental spectra are inevitably limited by time resolution (see Section 5.2), noise (the 50 Hz electric supply, the normal modes of the apparatus and less identifiable background noise) and external medium (such as the superimposition of solvent spectral features).

Some interpretations, for example, the association of frequencies with spectral lines, seem to refer only to discrete spectral features. In fact, we here again encounter some

tolerance depending on the observation scale: speaking of '*the* spectral line at a frequency ν_0' makes sense provided the width $\delta\nu$ of the peak of the spectrum $S(\nu)$ in $\nu = \nu_0$ is far smaller than the resolution $\Delta\nu \sim \nu^2\Delta t$ allowed by the experimental setup or computation accuracy. What appear to be purely monochromatic peaks might reveal an inner structure when unfolded by a higher resolution. Here also, the discrete or continuous character of a spectrum is an absolute property only for a given mathematical model of the real system, and should be reconsidered, together with its interpretation, when changing the scale of description or observation.

6. Discussion

6.1. *Singularities*

Discreteness is often, if not always, associated with *some kind of singularity*. For instance, any discrete shape A (or concrete body) exhibits a singularity at its boundary (which precisely defines the boundary):

$$\mathbf{1}(x) = 1 \quad \text{if} \quad x \in A \qquad \text{and} \qquad \mathbf{1}(x) = 0 \quad \text{if} \quad x \notin A. \tag{36}$$

Similarly, any countable partition $(A_j)_j$ (the sets $(A_j)_j$ having pairwise disjoint interiors) can be associated with a stepwise function $f_{|A_j} \equiv j$, which is discontinuous at each boundary δA_j, where it jumps from j to other integer values. We also see here a repetition of the leitmotiv of this paper: such a singularity is a *feature of the mathematical idealisation* of the system, which is of a different nature compared to the smooth 'physical' profiles: it physically turns into a smooth step at sufficiently small scales, and into a fuzzy boundary layer at still smaller ones. For all practical purposes, using step functions is to be preferred at larger observation scales (except in the case, discussed in Section 6.4, of a fractal boundary). *The physical smoothness is nevertheless to be borne in mind if we are to avoid falling into meaningless paradoxes.*

This point might even be expressed mathematically by modelling the boundary by a sigmoidal function

$$f_a(x) = \frac{1}{2}\,(\tanh(x/a) + 1) \tag{37}$$

smoothly interpolating between 0 and 1. This profile converges (in the sense of Schwartz distributions) towards a step function in $x = 0$ in the limit when the width a tends to 0 (see Figure 10):

$$\lim_{a\to 0} \frac{\tanh(x/a) + 1}{2} = \lim_{a\to 0} \frac{1}{1 + e^{-2x/a}} = \Theta(x) \equiv \begin{cases} 1 & \text{if} \quad x > 0 \\ 0 & \text{if} \quad x < 0. \end{cases} \tag{38}$$

Here, in $d = 1$, the Laplacian Δf_a is merely the second derivative

$$f_a''(x) = -2\sinh(x/a)\,[a(1 + \cosh(x/a))]^{-2},$$

which behaves as $-x/2a^3$ in the neighbourhood of $x = 0$ (more precisely, provided $|x| \ll a$) while remaining bounded when $a \to 0$ at fixed x. Hence the graph of Δf_a exhibits a marked feature, almost diverging to $\pm\infty$ when $a \to 0^{\mp}$, that indicates the

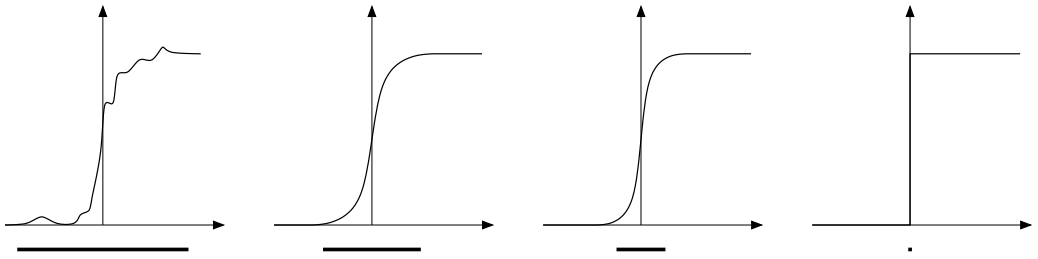

Fig. 10. Sketch of a boundary profile at different scales (the bar indicates a given interval $[-a, a]$). The three smooth profiles, accounting for the same physical feature observed at different scales, are to be contrasted with the mathematical idealisation (step-like profile) obtained in the limiting situation $a = 0$.

steep jump occuring there; the relief of the Laplacian is actually all the more marked as the jump is steep, that is, as a is small. Taking the limit $a \to 0$ induces a qualitative change: turning the generic situation $a > 0$ (even when it is very small) into the isolated value $a = 0$ is not innocuous. We here recover localisation arising in some limit (here $a \to 0$) and the associated singularities, reflecting the ideal character and different nature of this representation of a physical boundary. For instance, while it makes sense to add a small localised perturbation on the physical profiles and investigate its fate, the only perturbation of a step function (while remaining a step) is a translation of the discontinuity point.

In the above example, as in Section 3.6, Schwartz distributions allow us to give a mathematically well-defined meaning to the limit $a \to 0$, and to exchange derivation and the limit $a \to 0$, leading to $\Delta\Theta = \delta'$. It is then possible to investigate in a unified framework the stability of a step function with respect to superimposed fluctuations. *Schwartz theory thus reconciles, with all the desired mathematical rigor, discrete and continuous objects* and somehow smoothes out the debate.

More generally, the Laplacian $\Delta f(x)$ measures the difference between the value of f in x and its average in a neighbourhood of x. Namely, in $d = 1$,

$$\frac{1}{2}\,[f(x+h) + f(x-h)] - f(x) \approx \bar{f}_h(x) - f(x) \approx \frac{h^2}{2}\,\Delta f(x). \tag{39}$$

It thus vanishes if f is uniform or linear and it emphasises any localised inhomogeneity, bringing out a discrete feature in x from its surrounding $[x-h, x+h]$. In higher dimensions, taking the Laplacian of a shape brings out the discontinuity occurring at its boundaries, and thus delineates the edges of this shape, providing a basic tool for image analysis (Canny 1986).

6.2. *Singular limits and emergent properties*

We have just encountered in Section 6.1 a *singular limit* $a \to 0$ and realised the deeply differing nature of the limiting behaviour (here a discrete, discontinuous step, see Figure 10) compared with the behaviour for an arbitrarily small but finite value of a (a smooth step). Taking the limit $a \to 0$ induces a *qualitative gap*, from continuous to discrete, since there

is no way to recover a smooth profile starting from the discontinuous step. Moreover, the limit is not uniform, so it does not commute with other operations (derivation, for instance, or continuous dependence with respect to an auxiliary control parameter) except in the specially designed framework of Schwartz distributions. Such singular limits are ubiquitous in the interplay between discrete and continuous features. For example:

— The continuous limit $\epsilon \to 0$ of a partition in cells of linear size ϵ (or lattice of parameter ϵ).
— The classical limit $\hbar \to 0$ (rather $\hbar/A_c \to 0$ where A_c is the characteristic classical action scale).
— The thermodynamic limit $N \to \infty$.

Paradoxes arise when comparing and trying to relate the properties of finite systems to their limiting behaviour (Krivine and Lesne 2003). It is essential to bear in mind that the limit induces a qualitative change in the system behaviour, with an irreversible loss of information. If the system depends on another control parameter θ, it might happen that the limits $\epsilon \to 0$ and $\theta \to \theta_c$ do not commute, as a result of the singular nature of $\epsilon \to 0$. The way out of this follows from renormalisation-group ideas, which suggest we *take the two limits jointly*, according to the procedure: $\epsilon = a\epsilon_1$, $\theta = \theta_c + a^\alpha(\theta_1 - \theta_c)$ and $a \to 0$ at fixed ϵ_1 and θ_1. Typically, the joint limit is trivial except for a special choice of the exponent α, from which we get the full behaviour. More generally, joint rescalings often provide a powerful tool for capturing singular emergent behaviours (Lesne 1998).

6.3. *Digital computing*

The different causal nature of (ideal) digital computing, compared with the standard one, which is limited by rounding errors, is identified by computational mathematics (Longo 2002). In fact, from a physical viewpoint, computing *on an actual digital computer* is bound by an accuracy limitation of the same nature: computer elements are physical devices, experiencing external perturbations as well as unavoidable, intrinsic thermal noise (that is, noise originating in the thermal motion of atoms, which itself merely reflects their kinetic energy at thermal equilibrium). Strictly speaking, errors may arise, but in practice the probability is so low that they can be considered not to occur. This might be, for instance, due to a high activation barrier ΔF for taking paths other than the quasi-deterministically prescribed one: the characteristic time to observe the system wandering away can be roughly estimated as the Kramers time $\tau_K \sim e^{\Delta F/k_B T}$ (where k_B is the Boltzmann constant) (Hänggi *et al.* 1990), and this time increases exponentially if many such barriers line the 'deterministic' computation path.

Although impossible to detect in practice, this nuance is of importance: *improbability* and *impossibility* are not of the same nature, and no conceptual gap between continuous and digital computing arises if we stick to an improbability of observing a different result from the expected one in a digital computation. The same subtlety is encountered with the *emergence of irreversibility* and the associated Second Law of thermodynamics; similarly, paradoxes and dead ends appear when treating an improbability (that is, an event of probability smaller than the inverse age of the Universe) as a strict impossibility (that is,

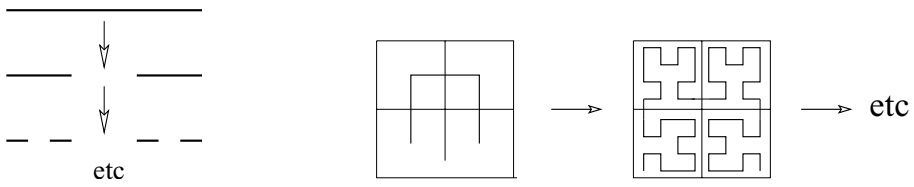

Fig. 11. (Left) lacunary Cantor set, of null measure and fractal dimension $d_f = \log 2/\log 3$ (Cantor 1883). (Right) convoluted plane-filling Hilbert curve, with $d_f = 2$ (Hilbert 1891).

an event of probability strictly equal to 0), and trying to derive rigorously the microscopic basis of this presumed impossibility of observing backward evolutions (Lebowitz 1993).

Theoretical computing on a Turing machine does not suffer such flaws: it achieves ideal digital computing, and hence is of a *deeply different causal nature* (Bailly and Longo 2004). This means that the real world does not work as a Turing machine, and that such an ideal machine, in a sufficiently long (but finite) time will always lose the imitation game (proposed by Turing to check the intelligence of machines), if played with actual physical systems, a human being, or a real computer (Turing 1950). Only the time required to discriminate the players will vary between these three protagonists of a Turing test.

6.4. *Fractals: at the border between discreteness and continuity*

Fractal geometry, initiated (among others) by Bouligand, Hausdorff and Minkowski (see, for instance, Gouyet (1996)) and popularised in physics and other natural sciences by Mandelbrot (see, for instance, Mandelbrot (1977a, 1997b)) might be seen as a hybrid of discrete and continuous features.

Let us first recall the definition of the main characteristic of a fractal structure: its *fractal dimension* d_f (Haursdorff 1919). It might either be:

Local – for example, the mass $M(r)$ contained in a ball of radius r scales according to $M(r) \sim r^{d_f}$; or

Global – for example, the number $N(\epsilon)$ of cells of linear size ϵ required to cover the fractal structure scales according to $N(\epsilon) \sim \epsilon^{-d_f}$.

In the case of a Cantor set (Figure 11, left), this notion of fractal dimension interpolates between the (integer) topological dimension of the underlying space and the vanishing dimension of a discrete (countable) set of points: so should we say this Cantor dust is discrete (although uncountable) or continuous (although of null measure)? And what about the plane-filling Hilbert curve (Figure 11, right)? The answer is conditioned by the observer himself: unlike the case of a normal 'Euclidean' body, the local density $\rho(r)$ now depends on the scale r of the observation: $\rho(r) \sim r^{d_f - d}$. In real systems (as you would expect), fractal geometry is an idealisation that breaks down at very small scales and very large ones, where Euclidean geometry rules again.

The fractal structure behaves in practice as a continuum if and only if $d_f = d$ (integer), for instance, a Brownian trajectory in the plane or the above-mentioned plane-filling Hilbert curve. In other cases, *fractal structures behave in their own fashion, which is neither discrete nor continuous.* They are often the spatial expression of a critical phenomenon,

where all scales participate in the behaviour and can no longer be separated; accordingly, the correlation length ξ diverges. This feature is reflected in the self-similarity of fractal structures. The spatial correlation function then exhibits a *power law behaviour* $C(r) \sim r^{d_f - d}$ (instead of the exponential decrease $C(r) \sim e^{-r/\xi}$ of the finite characteristic scale ξ). In fact, more generally, power laws might be seen as the signature of a *third category lying between the discrete and continuous*, as we have already encountered in spectra in Section 5.3.

Taking the continuous limit might be trivial, for example, when considering equally distributed discrete tags on a continuous shape or function. It might, on the other hand, be a puzzling task in the case where this limit is singular, that is, when a qualitative jump arises between the continuous system and its discrete counterparts. A typical example is the measuring of a fractal curve that requires a number of steps of diverging (in the case of a convoluted fractal structure with $d_f > 1$) or vanishing total length (in the case of a lacunary fractal structure with $d_f < 1$). The way out of this puzzle is to rescale jointly the stepsize a and the step number $N(a)$; the exponent involves the fractal dimension $N(ka) \sim k^{-d_f} N(a)$.

7. Conclusion

In conclusion, physics in all instances is an interplay between discrete and continuous features, mainly because any such feature actually characterises a *representation*, from a given observer, of the real system and its evolution. This extended 'relativity principle' implies that discrete and continuous modellings, behaviours or computing schemes are the inseparable sides of the same coin. Rather than motivating a debate about the reality of exclusively discrete or continuous pictures, observations of physical phenomena lead us to elaborate more complex categories, bridging discreteness and continuity: fractal structures, discrete features punctuating a continuum, or continuous behaviour smoothing out an accumulation of discrete events. In practice, the choice between discrete and continuous models should be based on a comparison between the respective scales of description, observation, variations (for example, gradient scales, oscillation periods, or inhomogeneity sizes) and correlations. In this way, it is possible to disentangle the joint discrete and continuous natures of any natural system in a 'subjective' fashion that is highly dependent on the specific phenomenon and experimental setup being considered. For instance, nowadays we know quite clearly how to determine when a photon should be described as a wave or as a point particle.

A key point is that *the discrete is not an approximation of the continuum nor the converse*. Great care should be taken when passing from discrete to continuous models and conversely, since their natures are irremediably different. Paradoxes and inconsistencies between discrete and continuous viewpoints only appear when we forget that our descriptions, and even physical laws, are only *idealised abstractions, tangent to reality in an appropriate scale range*, and unavoidably bounded above and below. As a result, wild and spurious features arise when we push a model beyond its validity range, and limiting behaviours exhibit emergent properties, of a qualitatively different nature, reflecting the singularity of the limit (continuous limits in the present case). Conversely,

coarse-grainings are also quite delicate and care should be taken to get closed effective descriptions, minimising the loss of relevant information and approximations. But both procedures (continuous limits and coarse-grainings) are at the core of theoretical physics, aiming at unifying all the different observations, descriptions and laws into a consistent, minimal explanatory frame capturing the multiple facets of the real world.

This point is subsumed in a more general one: any physical theory is at the same time based on a representation of the system and deals only with this representation, while reality always remains beyond the theory and is never fully captured. Hence, as already emphasised by Newton, and more recently in the context of irreversible thermodynamics (Chernov and Lebowitz 1997), the mathematical analysis of any physical model should be enlarged by an additional pragmatic status for the ensuing assertions, that of being *physically exact*. Indeed, since the model is only a plausible approximation of the real system, only robust and plausible features make sense, hence some tolerance of improbable events should be accepted: a property that fails to be observed only with a negligible property (at relevant scales) should be considered as true. *This opens a gap between mathematics and physical studies, which is essential to go beyond the mere analysis of a model and shift to an understanding of the real world.*

Acknowledgements

I wish to extend my warm thanks to M. Falcione, H. Krivine, G. Longo, J. Treiner and A. Vulpiani for numerous fruitful discussions and for their comments on a preliminary version of this paper.

References

Arnold, L. (1980) On the consistency of the mathematical models of chemical reactions. In: Haken, H. (ed.) *Dynamics of synergetic systems*, Springer-Verlag 107–118.

Auger, P. and Roussarie, R. (1994) Complex ecological models with simple dynamics: From individuals to populations. *Acta Biotheoretica* **42** 111–136.

Badii, R. and Politi, A. (1999) *Complexity. Hierarchical structures and scaling in physics*, Cambridge University Press.

Bailly, F. and Longo, G. (2004) Causalités et symétries dans les sciences de la nature. Le continu et le discret mathématiques. In: Joinet, J. B. (ed.) *Logique et interaction: pour une géométrie de la cognition*, Presses Universitaires de la Sorbonne, Paris.

Baker, G. L. and Gollub, J. B. (1996) *Chaotic dynamics: An introduction*, 2nd edition, Cambridge University Press.

Balian, R. (2004) Entropy, a protean concept. In: Dalibard, J., Duplantier, B. and Rivasseau, V. (eds.) *Poincaré Seminar 2003*, Birkhaüser.

Bensoussan A., Lions, J. L. and Papanicolaou, G. (1978) *Asymptotic analysis for periodic structures*, North Holland.

Berry, M. (2001) Chaos and the semiclassical limit of quantum mechanics (is the moon there when somebody looks?). In: Russell, R. J., Clayton, P., Wegter-McNelly, K. and Polkinghorne, J. (eds.) *Quantum mechanics: Scientific perspectives on Divine Action*, Vatican Observatory – CTNS Publications 41–54.

Boffetta, G., Cencini, M., Falcioni, M. and Vulpiani, A. (2002) Predictability: a way to characterize complexity. *Phys. Rep.* **356** 367–474.

Canny J. F. (1986) A computational approch to edge detection. *IEEE Transactions on Pattern Analysis and Machine Intelligence* **8** 679–714.

Cantor G. (1883) Über unendliche, lineare Punktlannigfaltigkeiten. *Mathematische Annalen* **21** 545–591.

Cardy, J. (2004) Field theory and nonequilibrium statistical mechanics. Lecture notes available online at `http://www.thphys.physics.ox.ac.uk/users/JohnCardy/home.html`.

Chernov, N. and Lebowitz, J. L. (1997) Stationary nonequilibrium states in boundary driven Hamiltonian systems: shear flow. *J. of Stat. Phys.* **86** 953–990.

Chopard, B. and Droz, M. (1998) *Cellular automata modeling of physical systems*, Cambridge University Press.

Cross M. C. and Hohenberg, P. C. (1993) Pattern formation outside of equilibrium. *Revs. Mod. Phys.* **65** 851–1112.

Dettmann, C. P. and Morriss, G. P. (1996) Proof of Lyapunov exponent pairing for systems at constant kinetic energy. *Phys. Rev. E* **53** R5545–R5548.

Diener, F. and Diener, M. (eds.) (1995) *Nonstandard analysis in practice*, Springer-Verlag.

Dorfman, J. R. (1999) *An introduction to chaos in nonequilibrium statistical mechanics*, Cambridge University Press.

Droz, M. and Pekalski, A. (2004) Population dynamics with or without evolution: a physicist's approach. *Physica A* **336** 84–92.

Eckmann, J. P. (1981) Roads to turbulence in dissipative dynamical systems. *Revs. Mod. Phys.* **53** 643–654.

Eckmann, J. P. and Ruelle, D. (1985) Ergodic theory of chaos and strange attractors. *Revs. Mod. Phys.* **57** 617–656.

Ernst, M. H. (2000) Kinetic theory of granular fluids: hard and soft inelastic spheres. In: Karkheck, J. (ed.) *Proc. NATO ASI on dynamics: models and kinetic methods for non-equilibrium many body systems*, Kluwer 239–266.

Falcioni, M., Vulpiani, A., Mantica, G. and Pigolotti, S. (2003) Coarse-grained probabilistic automata mimicking chaotic systems. *Phys. Rev. Lett.* **91** 044101.

Frisch, U. (1995) *Turbulence: The legacy of A. N. Kolmogorov*, Cambridge University Press.

Gardiner, C. W. (1983) *Handbook of stochastic methods*, Springer-Verlag.

Gaspard, P. (2004a) Maps. In: Scott, A. (ed.) *Encyclopedia of Nonlinear Science*, Taylor and Francis, London.

Gaspard, P. (2004b) Quantum theory. In: Scott, A. (ed.) *Encyclopedia of Nonlinear Science*, Taylor and Francis, London.

Gaspard, P. and Dorfman, J. R. (1995) Chaotic scattering theory, thermodynamic formalism and transport coefficients. *Phys. Rev. E* **52** 3525–3552.

Gaspard, P. and Wang, X. J. (1993) Noise, chaos, and (τ, ϵ)-entropy per unit time. *Phys. Rep.* **235** 321–373.

Ghil, M. and Mullhaupt, A. (l985) Boolean delay equations: periodic and aperiodic solutions. *J. Stat. Phys.* **41** l25–l74.

Givon, D., Kupferman, R. and Stuart, A. (2004) Extracting macroscopic dynamics: model problems and algorithms. *Nonlinearity* **17** R55–R127.

Gonze, D., Halloy, J and Gaspard, P. (2002) Biochemical clocks and molecular noise: Theoretical study of robustness factors. *J. Chem. Phys.* **116** 10997–11010.

Gouyet, J. J. (1996) *Physics and fractal structures*, Springer-Verlag.

Gruber, C., Pache, S. and Lesne, A. (2004) The Second Law of thermodynamics and the piston problem. *J. Stat. Phys* **117** 739–772.

Guckenheimer J. and Holmes, P. (1983) *Nonlinear oscillations, dynamical systems and bifurcations of vector fields*, Springer-Verlag.

Gutzwiller, M. C. (1990) *Chaos in classical and quantum mechanics*, Springer-Verlag.

Hänggi, P., Talkner P. and Borkovec, M. (1990) Reaction-rate theory: fifty years after Kramers. *Revs. Mod. Phys.* **62** 251–341.

Hausdorff F. (1919) Dimension und ausseres Mass. *Math. Ann.* **29** 157–179.

Hilbert D. (1891) Über die stetige Abbildung einer Linie auf ein Flächenstück. *Mathematische Annalen* **38** 459–460.

Jaynes, E. T. (1989) *Papers on probability, statistics and statistical physics*, Kluwer.

Kirkpatrick, T. R. and Ernst, M. H. (1991) Kinetic theory for lattice gas cellular automata. *Phys. Rev. A* **44** 8051–8061.

Kolmogorov, A. N. and Tikhomirov, V. M. (1959) ϵ-entropy and ϵ-capacity of sets in functional space. *Russian Mathematical Surveys* **2** 277–364. (Translated in *Translations Am. Math. Soc.* (1961) **17** 277–364; also available in Shiryayev, A. N. (ed.) (1993) in *Selected works of A. N. Kolmogorov*, Vol. III, Kluwer 86–170.)

Krivine, H. and Lesne, A. (2003) Mathematical puzzle in the analysis of a low-pitched filter. *American Journal of Physics* **71** 31–33.

Laguës, M. and Lesne, A. (2003) *Invariances d'échelle*, Series 'Échelles', Belin, Paris.

Landau, L. D. and Lifschitz, E. M. (1984a) *Theory of elasticity*, Pergamon Press, Oxford.

Landau, L. D. and Lifschitz, E. M. (1984b) *Hydrodynamics*, Pergamon Press, Oxford.

Landau, L. D. and Lifschitz, E. M. (1984c) *Electromagnetism of continuous media*, Pergamon Press, Oxford.

Lebowitz, J. L. (1993) Boltzmann's entropy and time's arrow. *Physics Today* **46** 32–38.

Lesne, A. (1998) *Renormalization methods*, Wiley.

Lind, D and Marcus, B. (1995) *An introduction to symbolic dynamics and coding*, Cambridge University Press.

Longo, G. (2002) Laplace, Turing and the 'imitation game' impossible geometry: randomness, determinism and program's in Turing's test. In: Conference on cognition, meaning and complexity, Univ. Roma II.

Ma, S. K. (1976) *Modern theory of critical phenomena*, Benjamin.

MacKernan, D. and Nicolis, G. (1994) Generalized Markov coarse-graining and spectral decompositions of chaotic piecewise linear maps. *Phys. Rev. E* **50** 988–999.

Mandelbrot B. (1977a) *Fractals: form, chance and dimension*, Freeman.

Mandelbrot B. (1977b) *The fractal geometry of Nature*, Freeman.

Mielke, A. and Zelik, S. (2004) Infinite-dimensional hyperbolic sets and spatio-temporal chaos in reaction-diffusion systems in $\mathbf{R}^n$ (preprint available at `http://www.iadm.uni-stuttgart.de/LstAnaMod/Mielke`).

Murray J. D. (2002) *Mathematical biology*, 3rd edition, Springer-Verlag.

Nicholson, C. (2001) Diffusion and related transport mechanisms in brain tissue. *Rep. Prog. Phys.* **64** 815–884.

Nicolis, G. and Gaspard, P. (1994) Toward a probabilistic approach to complex systems. *Chaos, Solitons and Fractals* **4** 41–57.

Nyquist, H. (1928) Certain topics in telegraph transmission theory. *AIEE Trans.* **47** 617–644.

Parry, W. (1981) *Topics in ergodic theory*, Cambridge University Press.

Poincaré, H. (1892) *Les méthodes nouvelles de la mécanique céleste*, Gauthiers-Villars, Paris.

Pollicott, M. and Yuri, M. (1998) *Dynamical systems and ergodic theory*, Cambridge University Press.

Rezakhanlou, F. (to appear) Kinetic limits for interacting particle systems. *Springer-Verlag Lecture Notes in Mathematics.*

Ruelle, D. (1986) Resonances of chaotic dynamical systems. *Phys. Rev. Lett.* **56** 405–407.

Ruelle, D. and Takens, F. (1971) On the nature of turbulence. *Commun. Maths. Phys.* **20** 167–192; *Commun. Maths. Phys.* **23** 343–344.

Schnakenberg, J. (1976) Network theory of microscopic and macroscopic behavior of master equation systems. *Revs. Mod. Phys.* **48** 571–585.

Shannon, C. E. (1948) A mathematical theory of communication. *The Bell System Technical Journal* **27** 479–423 and 623–656.

Shannon, C. (1949) Communication in the presence of noise. *Proceedings of the IRE* **37** 10–21. (Reprinted in *Proceedings of the IEEE* **86** 447–457 (1998).)

Stauffer, D. and Aharony, A. (1992) *Introduction to percolation theory*, Taylor and Francis, London.

Taniguchi, T. and Morriss, G. P. (2002) Stepwise structure of Lyapunov spectra for many-particle systems using a random matrix dynamics. *Phys. Rev. E* **65** 056202.

Thomas, R. and Kaufman, M. (2001) Multistationarity, the basis of cell differentiation and memory. I. Structural conditions of multistationarity and other non-trivial behaviour. II. Logical analysis of regulatory networks in terms of feedback circuits. *Chaos* **11** 170–195.

Turing, A. M. (1950) Computing machinery and intelligence. *Mind* **59** 433–560.

Turing, A. M. (1952) The chemical basis of morphogenesis. *Phil. Trans. R. Soc. London B* **237** 37–72. (Reprinted in Saunders, P. T. (ed.) (1992) *Collected works of A. M. Turing*, vol. 2, North Holland.)

Van Beijeren, H. and Dorfman, J. R. (1995) Lyapunov exponents and Kolmogorov–Sinai entropy for the Lorentz gas at low densities. *Phys. Rev. Lett.* **74** 1319–1322.

Vicsek, T. (ed.) (2001) *Fluctuations and scaling in biology*, Oxford University Press.

Werhl, A. (1978) General properties of entropy. *Rev. Mod. Phys.* **50** 221–260.

Zaks, M. and Pikovsky, A. (2003) Dynamics at the border of chaos and order. In: Livi, R. and Vulpiani, A. (eds.) *The Kolmogorov legacy in physics* 61–82.

Zurek, W. H. and Paz, J. P. (1995) Quantum chaos: a decoherent definition. *Physica D* **83** 300–308.